

**DEVELOPMENT OF A MAGNETITE TRACER
PROTOCOL FOR SEASONAL MEASUREMENT OF
BED SEDIMENT BIODIFFUSION COEFFICIENTS**

A Thesis

Submitted to the Graduate Faculty of the
Louisiana State University and
Agricultural and Mechanical College
in partial fulfillment of the
requirements for the degree of
Master of Science in Chemical Engineering

In

The Department of Chemical Engineering

by
Paul David Libbers
B.S., Louisiana State University, 1998
May 2002

Acknowledgments

Funding for this research was provided by the Gordon A. and Mary Cain Endowment to the chemical engineering department. I would like to thank the members of my graduate advisory committee for generously giving of their time and expertise: Dr. Louis Thibodeaux for his many great ideas and for helping me to develop my skills of “thinking outside of the box;” Dr. John Fleeger for generously allowing the use of his laboratory facilities and equipment, and for lending his expertise in the areas of benthic studies; Dr. Samuel Bentley for his time and for the great idea which eventually led to the design of the sampling equipment; Dr. K.T. Valsaraj for his support and interest in the project, and Dr. Danny Reible for the many suggestions for further research and refining the project. Without their knowledge and time this project would not have been possible. For my student workers, André Marquette and Angel Singleton, who spent long afternoons performing data analyses and braved the waters (and alligators) with me on Capitol Lake and Bayou Braud, I am forever grateful. I am also thankful for Xiaoxia Lu and Yunzhou Chai, whose knowledge of laboratory methods and oligochaete worms was indispensable. I would also like to thank my family for their support through this project and for putting up with many late nights and long weekends. Furthermore, I would like to thank the many students and researchers who came before me and paved the way for my research. Above all, I would like to thank my Lord and Savior, Jesus Christ, for making graduate school and this project a reality for me.

Table Of Contents

Acknowledgments	ii
Abstract	v
Chapter 1. Introduction	1
Chapter 2. Literature Review	5
2.1 Overview	5
2.2 Environmental Factors that Affect Bioturbation	6
2.3 Models of Bioturbation	8
2.4 Tracers Used to Track Sediment Processes	13
Chapter 3. Site Selection and Characterization	18
3.1 Overview	18
3.2 Capitol Lake	18
3.2.1 Sediment Analysis	20
3.2.2 Benthic Analyses	20
3.2.3 Taxonomic Classification	22
3.3 Bayou Braud	23
Chapter 4. Experimental Design and Procedures	26
4.1 Overview	26
4.2 Sediment Tracer Experiments	26
4.2.1 Establishment of Research Plots	27
4.2.2 Sampling Procedures	28
4.2.3 Core Extrusion and Slicing	31
4.2.4 Analysis of Core Sections	33
4.3 Fecal Matter Collection Experiments	34
Chapter 5. Presentation and Discussion of Results	37
5.1 Overview	37
5.2 Fecal Matter Collection Experiments	37
5.3 Presentation of Raw Data from Tracer Experiments	39
5.4 Data Analysis	43
5.4.1 Model Description	43
5.4.2 Initial Sample Profiles	43
5.4.3 Curve Fitting Procedures	45
5.5 Presentation of Results	50
5.5.1 Example Model Fits	50
5.5.2 Final Results of Tracer Experiments	52
5.5.3 Discussion of Final Results	56

Chapter 6. Conclusions and Recommendations	62
6.1 Conclusions.....	62
6.2 Recommendations	63
References	65
Appendix	69
A.1 Overview	69
A.2 Fecal Matter Collection Experiments	69
A.3 Initial Profile Experiments.....	70
A.4 Benthic Tracer Study Data	71
A.4.1 Experiment 1, Capitol Lake, December 2001	72
A.4.2 Experiment 2, Capitol Lake, January 2002	76
A.4.3 Experiment 3, Capitol Lake, February 2002.....	80
Vita	84

Abstract

This thesis describes the development of a particle tracer technique for making short-term, *in situ* measurements of aquatic bed sediment biodiffusion coefficients. The bioturbation process in the upper sediment layers of streams, lakes, estuaries, and the marine environment moves particles and porewater. When present, organic chemicals, metals, colloids, etc., are transported across these layers and exchanges may occur at the sediment-water interface. Fickian biodiffusion coefficients that characterize such particle movements, D_b (cm^2/yr), are used for assessing chemical diagenesis rates and contaminant fluxes and are specific to each site. Chemical Fate and Transport (CFaT) models, developed for tracking contaminants in aquatic environments, require a method of measuring the biodiffusion coefficient at specific locations. This measurement protocol should also be able to detect seasonal or other time dependent variations in the biodiffusion coefficient for improved model predictions. Magnetite, a tracer with a long historical use in scientific studies of porous media, particle transport, etc., was chosen. Unlike most of the other tracers used in this field, magnetite, an inexpensive and naturally occurring iron oxide, is readily obtained from ceramic supply companies and gives reasonable estimations of biodiffusion coefficients from short-term experiments. The steps in the protocol include deployment and retrieval of the tracer, magnetite separation and measurement, math model interpretation, and statistical treatment of data. Application of the technique was tested on South Capitol Lake, a manmade, freshwater lake located in Baton Rouge, Louisiana. The surficial sediment in this lake was found to contain a fairly large population of oligochaete worms in abundances of approximately 18 000 worms/ m^2 . Field deployments of magnetite were conducted in December 2001, January 2002, and February 2002, giving biodiffusion

coefficient values of $0.9495 \pm 0.2565 \text{ cm}^2/\text{yr}$, $0.4566 \pm 0.3314 \text{ cm}^2/\text{yr}$, and $0.6591 \pm 0.3876 \text{ cm}^2/\text{yr}$, respectively. Although the protocol was capable of *in situ* measurements, testing over one or more calendar years at this and other sites will be needed to determine if the magnetite tracer protocol can be used to detect changes in D_b with the seasons of the year.

Chapter 1

Introduction

During the latter half of the twentieth century, control and elimination of hazardous pollutants in the environment became a major world focus. Regulations backed by strict governmental enforcement and stiff penalties for noncompliance spurred industrial sources to implement costly treatment processes that greatly reduced the magnitude of pollution being emitted to the environment. However, the bed sediments of many bodies of water receiving industrial wastewater discharges retained organic and metal pollutants long after those treatment processes came online, thus effectively maintaining some concentration of pollutants in the water (Thibodeaux, 2002).

Before water quality can improve, contaminated bed sediments must undergo remediation to prevent pollutants from being transported back to the water. Often remediation options include monitored natural recovery, *in situ* containment (i.e. capping with a thin layer of clean sediment), or dredging followed by *ex situ* treatment. Before selection of the optimal treatment plan is possible, often it is necessary to study and model the natural recovery process at work in bed sediments and its effect on water and biota quality (Thibodeaux, 2002). These models, known as Chemical Fate and Transport (CFaT) models, are based on physical, chemical, and biological processes naturally occurring at the sediment-water interface.

Traditionally, CFaT models tracked sediment-bound contaminants as they were released to the aqueous phase during particle resuspension processes such as occurs during storm events, dam removals, dredging, boating, etc. However, recent data suggests that these models greatly underestimate the magnitude of chemical releases between these

events. Such releases are believed to be enhanced by the presence of macroscopic infauna in the upper layers of the sediment bed. Therefore, recent models consider the bulk movement of sediment in the upper sediment layers and resistance to transport across the water-side boundary layer as two separate processes occurring in series. These models correlate the available laboratory data and may provide flux algorithms for use in CFaT models useful for predicting future conditions in both the sediment and the overlying water (Thibodeaux *et. al.*, 2001).

As mentioned above the most recent CFaT models show the overall flux of contaminants across the sediment-water interface as a function of both resistance at the benthic boundary layer and transport through the upper sediment layers. One such two-resistance model takes on the following form:

$$\left[\frac{N}{(C^* - C_w)} \right] = K_w = \frac{1}{\frac{1}{\beta} + \frac{h}{D_b K_d \rho_b}} \quad (1.1)$$

where: K_w = the overall mass-transfer coefficient, (cm/day)

N = the contaminant flux from the sediment, (mg/cm²·day)

C^* = the contaminant concentration in sediment pore water, (mg/cm³)

C_w = the contaminant concentration in the overlying water, (mg/cm³)

β = the water-side benthic boundary layer mass-transfer coefficient, (cm/day)

h = the average depth of origin of particles, (cm)

D_b = the biodiffusion coefficient for the sediment, (cm²/day)

K_d = the sediment-water partition coefficient for the contaminant, (cm³/mg)

ρ_b = the bulk dry density of bed solids, (g/cm³)

The second term in the denominator of the right-hand side of this equation quantifies sediment particle movement as a result of the bioturbation process. This phenomenon, which involves particle reworking and porewater flushing by benthic organisms present in the sediment, is responsible for sediment-bound contaminant movement from depth to the sediment-water interface. Although other models may more closely account for animal activities, the Fickian diffusion approach is very utilitarian and is supported by extensive data derived from radioisotope and other particle tracer studies fitted to diffusion models (Thibodeaux *et. al.*, 2001).

Estimation of benthic boundary-layer mass transfer coefficients(β) has been successfully carried out at seafloor sites using gypsum dissolution rates from alabaster plates (Santschi *et. al.*, 1991). Results of the study agreed within 15% and correlated well with theoretical relationships. Unfortunately, existing methods for measuring biodiffusion coefficients are often either expensive, lacking in accuracy, or both. The objective of this research is to develop and test a technique for *in situ* measurement of biodiffusion coefficients in bodies of water that is inexpensive, accurate over a short time period of weeks to months, and which is relatively easy to employ. In order to accomplish these goals, we have developed a technique using magnetite, a readily available magnetic mineral, as a particle tracer to quantify sediment reworking rates in water bodies.

The use of magnetite as a particle tracer in bed sediments is not a new idea. Apparently, it has been used on a routine basis for decades in various studies and experiments by researchers both in the laboratory and in the field. However, despite a strong oral history of its use, the literature is surprisingly silent on the subject, particularly the subject of techniques, advantages, disadvantages, protocols of deployment and use, etc.

Apparently it was supplanted in the early days of diagenetic studies by natural and artificial radiotracers, which arrive at the sediment-water interface without the need for deliberate application. Such radionuclides as ^{234}Th , ^7Be , ^{210}Pb , and ^{137}Cs presently receive widespread usage as particle tracers. In general, based on their decay half-lives, most of the members of this group integrate the particle mixing process over many months to years, some over many decades. Only ^7Be and ^{234}Th , with their short half-lives of 53.3 days and 24.1 days, respectively, have the ability of quantifying the short-term mixing process. However, this ability is dependent on a timely, atmospherically generated source for its delivery to the sediment-water interface. This sporadic delivery process renders its timely and consistent use very problematic for the routine parameter measurement needs of the current generation of CFaT models. Based on this evaluation and an extensive literature review for other, more appropriate tracers, magnetite was rediscovered and chosen for use in this research project. It forms the basis of a routine protocol for measuring values of biodiffusion coefficients (D_b) for use in equation 1.1 or similar CFaT models.

Chapter 2

Literature Review

2.1 Overview

At one time the resuspension of contaminated sediments in the water column was believed to be the only event of significance to the pollutant release process. However, models based on this premise failed to properly account for contaminants released between storm events. This release process problem necessitated modelers to calibrate soluble release transport rate coefficients based on concentration and flow data from the site. The process mechanism for soluble releases is one by which contaminated particles and porewater are moved upward through the sediment bed by bioturbation, a process in which organisms indigenous to the sediments move particles through feeding and locomotive activities. Once the particles reach the sediment-water interface, contaminants desorb from the particles into the water at the interface. Transport through the benthic boundary layer completes the release to the overlying water column. Although particle resuspension events account for a significant portion of the overall release of contaminants to the water column, CFaT models that properly combine time periods with their respective coefficients suggest that more mass is transported to the water column as a result of soluble releases (e.g. Limno-Tech, Inc., 1999; TAMS Consultants, Inc., 2000; Connolly *et. al.*, 2000; Blasland, Bouck & Lee, Inc., 2000). The soluble release fraction appears to be highly significant, accounting for nearly 30% of the total release in one study of the Lower Fox River (Thibodeaux, *et. al.*, 2001). Because of the hypothesized importance of bioturbation to the fate and transport of contaminants from the sediment bed to the overlying water column through measurements, it is necessary to gain further insight into the environmental factors that define and control

this process. Additionally, mathematical models of bioturbation will be evaluated and details of existing tracer techniques used for estimating model parameters will be reviewed.

2.2 Environmental Factors that Affect Bioturbation

It has been shown that different modes of feeding and locomotion demonstrated by benthic organisms have a high impact on the degree of sediment mixing on short-term time scales (Fornes *et. al.*, 1999). Functionally similar groups or species of organisms, known as guilds, can be classified according to three dichotomies: epifaunal/infaunal, mobile/stationary, and deposition/suspension feeding (Lee and Swartz, 1980). Epifaunal species reside at the surface, although they sometimes do burrow into the sediment. Infaunal species reside at depth in the sediment. Mobile species include organism that burrow into the sediment by displacing particles to create temporary burrows (“vagile” fauna) and organisms that construct semi-permanent or permanent burrows (“excavators”). Stationary organisms only move when threatened or to reproduce. Suspension feeders glean food particles from the water column above the sediment whereas deposit feeders ingest particles in the sediment layers. Of particular interest to this study is a group of semi-stationary, subsurface deposit feeders known as conveyer belt species because they contribute highly to the rate of sediment and porewater bioturbation and are relatively abundant in freshwater lakes and marshes (such as those in which this research was conducted). These species ingest sediments at depth and defecate on the surface, providing a conveyer belt-like process that exposes buried sediments and effectively covers surface sediments (Lee and Swartz, 1980). Examples of each group can be found in Lee and Swartz (1980). Additionally, Swift (1993) proposed a useful scoring system for ranking the relative contribution of each organism to the overall bioturbation process.

Many environmental factors have been investigated by experiments in the recent literature. Plainly, the extent to which bioturbation occurs is dependent upon the density of organisms in a given field site. Several studies (e.g. Benninger *et. al.*, 1979; Tedesco and Aller, 1997) showed that the presence of existing burrows (such as those excavated and abandoned by crustaceans) serve to move surface particles to depth since such burrows preferentially fill by the sloughing of surface sediments rather than the collapse of sediments from tube walls. Self and Jumars (1978) found that organisms selectively ingest particles based on particle size, surface texture, and specific gravity. Another important consideration towards particle selectivity is the availability of organic and microbial food sources on the surface of particles (Meadows and Anderson, 1966). Although some studies have supported this theory (for example, Smith *et. al.*, 1993), a study done by Fornes *et. al.* (1999) showed that benthic organisms had little or no preference amongst phytoplankton (algae), normal sediment, and smooth glass beads. Another factor investigated is preferential selection based on the size of particles. Wheatcroft (1992) showed that the distribution of fine particles tended to show a broader range than the distribution of larger particles having the same characteristics. Although the reason for this selectivity is not entirely discernible, the investigators believed that the case was preferential ingestion of fine particles by deposit feeders. Mazik and Elliott (2000) found that the degree of bioturbation increased in estuarine intertidal mudflats with a decrease in chemical pollution levels in the sediment. Swift (1993) found that sediment type does not clearly define the guilds of organisms present in a given area. Henderson *et. al.* (1999) showed that the mixing rate and maximum particle penetrations caused by bioturbation decrease as water depth increases in deep marine environments.

One additional consideration is the seasonal dependence of environmental factors and their effects on bioturbation. For example, organism abundance is influenced by availability of food sources, dissolved oxygen content, temperature, and frequency of storm events. Martin and Sayles (1987) found that warm-season average mixing rates in Buzzards Bay, MA were three times greater than cold-season rates, measured monthly over nearly two complete yearly cycles. Because this seasonal variability in mixing rates exists, an ideal method for measuring such rates would be based on a short enough time scale (weeks to months) as to measure such seasonal variations accurately.

2.3 Models of Bioturbation

Several mathematical models of the bioturbation process are found in the literature. Some models attempt to describe bioturbation using a general diffusion analog, while others attempt to account for modes of bioturbation specific to various organisms (e.g. Choy and Reible, 2000; Mohanty, 1997; Berner, 1980). The starting point of many of these models comes from the general diagenesis equation (Berner, 1980):

$$\frac{\partial c(z,t)}{\partial t} = \frac{\partial}{\partial z} \left[D_b(z,t) \frac{\partial c(z,t)}{\partial z} - \omega(z,t)c(z,t) \right] + \Sigma R(c,z,t) \quad (2.1)$$

where: c = concentration of a particulate tracer or pollutant, time- and depth-dependent

D_b = diffusion coefficient used as an eddy diffusivity plus any other pertinent diffusion processes

ω = advective velocity, often due to sedimentation

ΣR = sum of other sinks and sources

Here, the term in brackets is equivalent to the flux of particulate tracer or pollutant through the sediment. Many models in the literature are formed from this basic equation after

applying various simplifying assumptions, boundary conditions, and initial conditions. Only three of these that have application to conveyor-belt species will be considered here.

One model especially applicable to conveyor belt species was used successfully by Rice (1986). This model follows similar simplifications as the steady-state compaction equation formulated by Berner (1980), having additional terms for mass moved discretely by conveyor belt species. The following relations are used to simplify:

$$\omega(z, t) = \omega_i(z, t) + \omega_B(z, t) \quad (2.2)$$

$$c(z, t) = \rho[1 - \phi(z, t)]c_m(z, t) \quad (2.3)$$

$$\Sigma R = -\hat{B}(z, t)r(t) \quad (2.4)$$

$$\bar{B} = \int_l^L \hat{B} dz \quad (2.5)$$

where: ω_i = allochthonous burial component

ω_B = bioadvective burial component

ρ = average particle density, assumed constant

ϕ = porosity of bed

c = concentration of total solids in sediment bed

c_m = mass of particulate per mass of solids

r = particle egestion rate, (g particle/g biomass · day)

\hat{B} = distribution of biomass over mixed depth.

l, L = top and bottom of the biomass feeding zone

\bar{B} = total biomass inventory per unit area

Further, we assume random diffusion is negligible ($D_b = 0$), \bar{B} is constant with time, ω_{i0} (the advective velocity at the surface due to sedimentation) is constant, biomass is normally distributed about an axis $z = \bar{z}$ with a standard deviation σ , and the following boundary conditions:

$$\text{At } z = 0, \omega_0 = \omega(0, t) = \omega_{i0}(t) + \omega_{B0}(t), \phi = \phi_0 = \text{constant} \quad (2.6)$$

$$\omega_{B0}(t) = \frac{\bar{B}r(t)}{\rho[1 - \phi_0]} \quad (2.7)$$

Then, the final equation for overall advective velocity in the sediment at steady-state is found to be the following:

$$\omega(z, t) = \omega_{i0} \frac{1 - \phi_0}{1 - \phi(z)} + \frac{\bar{B}r(t)}{2\rho[1 - \phi(z)]} \text{erfc}\left(\frac{z - \bar{z}}{\sigma\sqrt{2}}\right) \quad (2.8)$$

where: erfc = complementary error function (tabulated in many statistical handbooks)

Here, the advective velocity is dependent upon the adjustable parameter and function values of \bar{z} , σ , and $\phi(z)$ measured for the specific site. Using the same assumptions and conditions, the solution for a radioactive tracer bound to particulates and undergoing only conveyor belt bioadvective mixing is given as:

$$\frac{\partial c}{\partial t} = -\frac{\partial}{\partial z}(\omega c) - \frac{\hat{B}(z, t)r(t)}{\rho[1 - \phi(z, t)]}c - kc$$

where: k = radioactive decay constant, time^{-1}

This equation closely modeled the actual velocity-depth profiles for two cores in Rice's (1986) experiment. However, any effects resulting from other mixing events or from flow in the horizontal direction were unaccounted for and, therefore, it was difficult to interpret overall rates of mixing from such bioadvective velocity profiles.

Recently, Aller (2001) presented a model that accounted for sources and sinks not at the sediment-water interface (e.g. burrow tubes within the sediment deposits subject to irrigation by overlying water). This model, known as the nonlocal exchange model, accounts for solute exchange with such intrasediment sinks in the reaction term as:

$$\left(\frac{\partial c}{\partial t}\right)_{irrigation} = \eta(c_B - c_s) \quad (2.9)$$

where: η = an adjustable exchange coefficient or nonlocal transport coefficient

c_B = concentration of solute in the burrow or other reservoir

c_s = concentration in sediment

Accounting for porosity changes with depth, and assuming an unreactive species, the compaction equation becomes:

$$\frac{\partial c}{\partial t} = \frac{\partial}{\partial z} \left[\phi D_b \frac{\partial c}{\partial z} - \omega \phi c \right] + \eta \phi (c_B - c) \quad (2.10)$$

Functional forms of η are then found from a best-fit solution of equation (2.9) using solute concentration-depth profiles.

One disadvantage this model has is that analytical solutions are often exceedingly tedious, when available. Also, it is necessary to have *a priori* porosity profiles for the sediment in question, which are difficult to measure and often vary greatly over even small spatial scales in sediment beds because they are largely a function of benthic organism density. Although a useful model for long-term experiments, the amount of data and numerical computation required to fit this model make it unattractive for short-term diffusivity calculations.

As previously mentioned, some models attempt to model bioturbation as a complex interaction of various processes occurring simultaneously in the sediment (e.g. Mohanty,

1997). Even though analytical solutions are generally available for these models and physical parameters can be easily estimated, use of these equations is restricted to organisms which feed and move according to the constraints of the equation. One approach to modeling the complex interactions amongst various benthic organisms and conditions present in bed sediments is to use a diffusive analogue instead of attempting to model the actual processes at work (Goldberg and Koide, 1962). Although this approach does not give insight into how bioturbation occurs, it does quantify the overall effects reasonably well in many cases using an eddy diffusion parameter, D_b , also called a biodiffusion coefficient. Although many experiments investigating the long-term effects of bioturbation on sediments include sedimentation (for example, Smith and Schafer, 1984; Gerino *et. al.*, 1994; Henderson *et. al.*, 1999), several studies suggest that for quiescent bodies of water sedimentation can be neglected (Wheatcroft, 1992; Gerino, 1990). In the absence of other sources and sinks (assume a nonreactive species) the model equation simplifies to:

$$\frac{\partial c}{\partial t} = D_b \frac{\partial^2 c}{\partial z^2} \quad (2.11)$$

The obvious advantage of such a model is the relative simplicity with which one can obtain analytical solutions to it. For example, many studies use a plane source with uniform loading, M , at $z = 0$ as an initial condition. For a semi-infinite slab, the solution to this model given by Crank (1976) is as follows:

$$c(z, t) = \frac{M}{\sqrt{\pi D_b t}} \exp\left(\frac{-z^2}{4D_b t}\right) \quad (2.12)$$

Regression of concentration-depth profile data for a known loading and time yields values for the biodiffusion coefficient. However, it is necessary to discard subsurface concentration peaks caused by conveyor belt species in calculating D_b since they are not part

of the diffusive mixing process (Fornes *et. al.*, 1999). Because of its historical data record, simplicity of use, and the ease at which data necessary for regression can be obtained, this model will be used for these experiments.

2.4 Tracers Used to Track Sediment Processes

A variety of tracers have been reported in the literature for quantifying the particle mixing processes in sediments. Because these diagenetic processes are key factors in chemical mobility in and from the bed, it is important to quantify the degree to which they occur. Specifically, this research is concerned with measurement of D_b , the biodiffusion coefficient, in various sediments and during various seasons of the year. Ideally, such a tracer will be easy to apply and detect in the bed, appropriate for short-term measurements, readily available, and cost effective. Tracers used in the literature for similar research will first be examined and then the tracer chosen for this study will be presented.

Traditionally, researchers have used various radioactive nuclides as tracers in sediment studies. These tracers are either naturally occurring or products of nuclear fallout (e.g. ^{238}U , ^7Be) or are widespread in the environment (e.g. ^{137}Cs). Radioactive tracers are classified as either short-lived (half-life on the order of days to months) or as long-lived (half-life on the order of years to centuries). Use of short-lived radioactive nuclides also necessitates the addition of a reaction and/or source term to the general balance equation to account for production from a parent molecule (if applicable) and radioactive decay.

Short-lived radionuclides have half-lives which are short enough that diffusional mixing timescales are of the same order of magnitude as radioactive decay processes in the sediment, resulting in an exponential activity with depth from which mixing rates can be determined (Henderson *et. al.*, 1999). ^7Be , a naturally occurring radiotracer ($t_{1/2} = 53.3$

days), is formed in the atmosphere by cosmic ray spallation of nitrogen and oxygen, which is then delivered to the air-water interface via wet and dry deposition. Once in the water column, ^7Be sorbs strongly to suspended solids and is deposited at the sediment-water interface by particle deposition (Fitzgerald *et. al.*, 2001). Rice (1986) used ^7Be to quantify mixing rates in the sediment of Lowes Cove, Maine. He successfully fit ^7Be activity-depth profiles to a model similar to equation 2.1, where the ΣR term was modeled as a first-order decay, to obtain values of D_b . Aller and Cochran (1976) proposed that measuring the activity of ^{234}Th ($t_{1/2} = 24.1$ days) in excess of the amount supported by ^{238}U would give valuable insight into biological and physical reworking activities in sediments. However, Aller *et. al.* (1980) noted that activity profiles were assumed to be at steady-state for calculation purposes. If this were a bad assumption, then D_b values calculated by this method may not truly represent D_b for the sediment. Martin and Sayles (1987) used a similar approach for $^{234}\text{Th}/^{238}\text{U}$ disequilibrium curve fits that gave good results. $^{222}\text{Rn}/^{226}\text{Ra}$ disequilibrium was also measured to estimate overall porewater diffusivity. Kershaw *et. al.* (1984) examined sediment near a nuclear facility's wastewater discharge zone to measure ^{241}Am , ^{244}Cm , and ^{242}Cm concentrations in addition to $^{239,240}\text{Pu}$ and ^{238}Pu , with longer half-lives. However, only qualitative observations were made as to the effect of bioturbation on these profiles and no mixing coefficients were calculated. Although such short-lived tracers are available (usually naturally occurring or nuclear fallout products) and useful for short timescale experiments, techniques for analyzing profiles require costly equipment and difficult parameter measurements.

Activity-depth profiles of long-lived radioactive nuclides are useful for measuring the depth of the mixed layer. Because these molecules are resident for periods of years

before significant decay, they become well mixed in the upper sediment and the depth at which they commence to decline is taken as the thickness of the mixed layer (e.g. Henderson *et. al.*, 1999; Benninger *et. al.*, 1979). Additionally, deliberate tracers (i.e. not naturally occurring) with long half-lives can give excellent short-term mixing quantifications by assuming the decay term is negligible in models. Benninger *et. al.* (1979) used ^{210}Pb ($t_{1/2} = 22.3$ yrs.) profiles to show the relative zone in which mixing occurs, indicating an exponential decay from 2-4cm down to approximately 15cm. Smith and Schafer (1984) used ^{210}Pb profiles to fit the diffusional model for 3-dimensional characterization of biological mixing on continental slope sediments of Newfoundland. This is possible because mixing rates are on the same time scale as the half-life of ^{210}Pb . Multi-dimensional measurements are necessary due to the largely heterogeneous distribution of biomass within the upper sediment zone. Henderson *et. al.* (1999) again uses ^{210}Pb to quantify mixing rates and mixing depths for various sea depths off of the Little Bahamas Bank. Robbins *et. al.* (1979) used ^{137}Cs ($t_{1/2} = 30$ yrs.) as a deliberate tracer to quantify bioturbation in *ex situ* experiments using freshwater sediments inoculated with oligochaete worms and one species of amphipod. Values of biodiffusion coefficients were calculated with the assumption that decay is negligible compared to bioturbation rates. Also, this experiment showed that rates of bioturbation are two to three orders of magnitude faster than molecular diffusion rates. Although well-suited for scientific research of biodiffusion processes, long-lived radioactive nuclides are difficult to use *in situ* and require expensive analytical equipment; thus, they are problematic for routine use in measuring biodiffusion coefficients in lakes or other bodies of water.

Another tracer common in the literature is a small particle called a luminophore. These tracers are produced by staining sand grains with a dye visible under ultraviolet light. The resulting tracers can be quantified by tedious counting under a microscope using an ultraviolet light source. Mahaut and Graf (1987) used luminophores to give rough quantifications of sediment displacement on a monthly time-scale. Gerino (1990) made a rough attempt to quantify biodiffusion coefficients with luminophores, and then in later experiments (Gerino *et. al.*, 1994) used a combination diffusion-advection model to fit luminophore count-depth curves with biodiffusion coefficients and advective velocities (ω) with good success. Mazik and Elliott (2000) measured decreases in biodiffusion coefficients with increasing sediment pollution levels using luminophores. Although successful in obtaining good experimental results, luminophores are not easily obtained since details of their preparation are currently protected by patent. Also, because skeleton and shell fragments present in the sediment are visible under ultraviolet light, tedious visible counting must be conducted under a microscope (Mahaut and Graf, 1987).

Several studies have made use of exotic particle tracers for studying animal-sediment dynamics. Carey (1989) introduced a plastic particle tracer that is close in size to actual sediment. These particles are then colored with fluorescent paint that can be detected fluorometrically. Wheatcroft (1992) used various sized glass beads to investigate the potential for particle size-dependent bioturbation in sediments. Fornes *et. al.* (1999) used phytoplankton, slope sediment, and glass beads tagged with radiotracers to determine the importance of food availability on particle selectivity in the sediment. Because these tracers received limited use in experiments, information on their availability and quantification is not well defined, and they will, therefore, not be considered for this research.

Recently, researchers developed a particle tracer technique that uses noble metals to label various size fractions of sediments (Olmez *et. al.*, 1994). This technique thermally diffuses gold and silver into sieved sediment particles, which can then be detected using instrumental neutron activation analysis (INAA). The technique was used successfully in Massachusetts Bay to quantify particle size-dependent bioturbation in sediments (Wheatcroft *et. al.*, 1994). However, tracer materials are expensive and not readily available. Equipment for analysis is highly specialized and, thus, not practical for the purposes of this research.

In selecting an appropriate tracer, suitability was determined based on cost of materials, availability, ease of use and detection, and capability to give results over time scales of weeks to months. Magnetite, a naturally occurring, readily available, iron mineral, was found to possess all of these characteristics. Analysis is accomplished by physical separation from dried sediment via magnet. Also there is usually no background concentration in most sites, although the presence of low levels of magnetite at sites will not hamper the technique since a background subtraction procedure is employed so that site concentration profiles reflect only the addition of fresh magnetite. In this research a magnetite tracer protocol for measuring biodiffusion coefficients used in CFaT models has been developed.

Chapter 3

Site Selection and Characterization

3.1 Overview

Several factors were considered when selecting appropriate sites in which to conduct research. Primarily, a site with fairly soft sediment that would be straightforward to obtain samples from, but which would maintain its structural integrity during analysis, was desired. Additionally, it was necessary for the site to have a well-established benthic community and a relatively quiescent overlying water column. Secondary considerations included distance between the site and our laboratory, accessibility of the site by boat, the depth of the water column, and the amount of boat traffic in the area. Two sites were rejected before the final research sites were selected: one due to accessibility problems (Bayou Manchac), and the other due to a lack of soft sediments (Thibodeaux Lake, a small lake just southwest of Baton Rouge). The final sites chosen were Capitol Lake in downtown Baton Rouge and Bayou Braud just south of Baton Rouge in Ascension Parish. These sites were conveniently located less than an hour from our laboratories, had favorable sediment textures, and gave good results from preliminary benthic analyses. Ultimately, however, only the Capitol Lake site proved to be acceptable for conducting experiments, as discussed later in this chapter. Details of these sites are given in the sections that follow.

3.2 Capitol Lake

Capitol Lake is a large lake located in downtown Baton Rouge on the grounds that includes the State Capitol building (see Figure 3.1). At one time, the lake was used as a wastewater receiving body by Westinghouse Corporation and as a drainage basin from adjacent facilities and roads. As a result, the lake became contaminated with

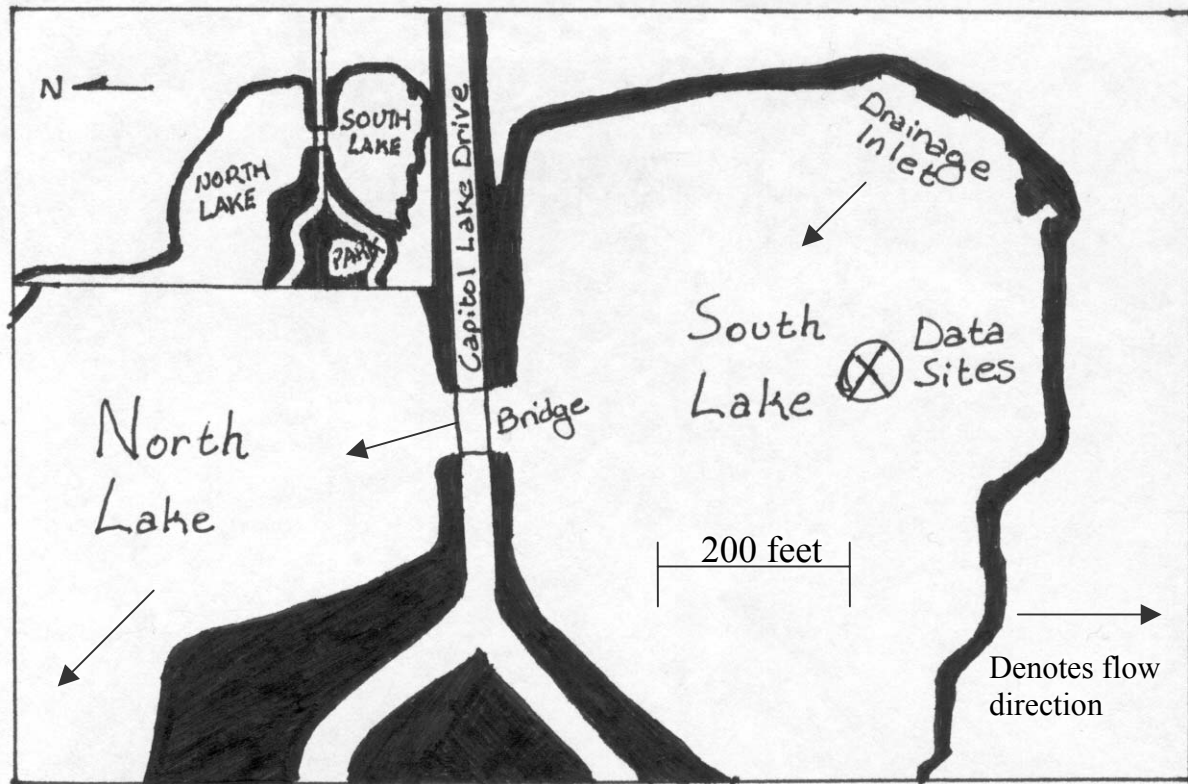


Figure 3.1 Vicinity and Detailed Map of the South Capitol Lake Site

polychlorinated biphenyls (PCBs) and heavy metals found in many of the products stored and produced in these facilities, although the exact source of contamination has not been conclusively determined (Myers and Poché, 1988). Geographically, the lake is split into two parts by a road between the State Capitol building and the Governor's Mansion. Because the pollution source was likely located at the northern end of the lake, the southern end of the lake was chosen to conduct research on, a smaller lake known as South Lake. This lake, 270 m by 150 m, is easily accessible by boat, shallow enough to obtain samples from (approximately 1.3 m deep), and has virtually no other boat traffic. Flow into South Lake occurs via Northdale Canal, which enters from the East. A deep scour zone appears near the inlet with a deltaic sediment fan beyond. The water flow continues through the bridge and into the main portion of Capitol Lake. Water level in the two lake system is maintained by a

pump station located on the western shore of Capitol Lake. The two lake system is clearly a depositional zone and dredging is planned; however, the presence of PCBs in the sediment has hampered these efforts. Despite the flow through South Lake, the water is nearly always quiescent, has characteristically warm temperatures that are almost uniform through the depth of the water column, and has an abundance of organic food sources to sustain benthic organisms due to trees and plants in the immediate vicinity.

3.2.1 Sediment Analysis

Qualitatively, South Lake sediment is a dark brown to black color with a fairly high porosity due to trapped gas pockets, probably resulting from methane gas production by anaerobic sediment-phase reactions. Although the sediment texture is soft, water content is low enough that retrieved cores can hold their shape during extrusion and slicing procedures. When disturbed, the sediment also emits a characteristic oil or petroleum odor. Quantitatively, a particle size analysis reveals that the sediment is classified as a silty loam, composed of 14.9% sand ($>50\ \mu\text{m}$), 68.9% silt ($2\ \mu\text{m}$ – $50\ \mu\text{m}$ range), and 16.2% clay (less than $2\ \mu\text{m}$ range).

3.2.2 Benthic Analyses

A preliminary benthic analysis conducted at the Capitol Lake site revealed that there was an adequate density of bioturbating species to conduct experiments there. Initially, five replicates, each 5 cm diameter cores approximately 6 cm deep, were taken from South Lake. Fixation was achieved by mixing the retrieved sediments with a solution of 10% buffered formalin and Rose Bengal vital stain for ease of differentiation between organisms and debris. Samples were fixed in this manner for 7–10 days prior to analysis. We then passed samples through a series of three sieves to retain organisms: a 1-mm coarse sieve to

Table 3.1 Preliminary Benthic Analysis of South Lake (August, 2001)

Sample	Count on Large Sieve (>1 mm)	Count on Small Sieve (<1 mm)	Total Count	Abundance Of Large Organisms (worms/m²)	Abundance Of Small Organisms (worms/m²)	Overall Organism Abundance (worms/m²)
Core 1	7	11	18	3 900	6 200	10 100
Core 2	3	9	12	1 680	5 050	6 740
Core 3	2	5	7	1 120	2 800	3 900
Core 4	14	10	24	7 860	5 610	13 480
Core 5	3	1	4	1 680	560	2 250
Overall	5.8	7.2	13	3 260	4 040	7 300

retain large organisms, a 500- μm sieve, and a 250- μm fine sieve to retain small organisms.

Organisms retained on the 1 mm sieve were counted separately from those on the smaller sieves because this size class represents the most significant bioturbation contributors. All significant bioturbating species found in Capitol Lake were species of tubificid oligochaete worms. Results for these counts are given in Table 3.1 along with estimated abundances.

Oligochaete worms retained during these analyses were stored in 70% ethanol for later inspection.

Although the preliminary benthic analysis for South Lake provided enough information to verify its suitability for conducting research, a more detailed analysis was later conducted to give accurate benthic organism counts in the sediment. Procedures for the analysis were the same as before, excepting that samples were retrieved using a 15 cm. square Eckman sampler. Again, the sample depth was approximately 6 cm since the estimated bioturbation mixing depth of sediment in freshwater environments is at most 6 cm as reported by many previous studies (e.g. Guinasso and Schink, 1975; Robbins *et. al.*, 1977; Officer and Lynch, 1982). Also, the fine-sized 250- μm sieve was no longer used, due

to an insignificant number of species retained on it during the preliminary benthic analysis, and a 2-mm sieve was used to remove coarse screenings and facilitate

Table 3.2 Detailed Benthic Analysis of South Lake (January, 2002)

Sample	Sample 1	Sample 2	Sample 3	Sample 4	Overall
Count large worms (> 1 cm)	188	190	224	202	201 ± 17
Count medium worms (> 5mm, < 1 cm)	173	154	201	179	177 ± 19
Count small worms (< 5 mm)	55	63	28	57	51 ± 16
Total Count	416	407	453	438	429 ± 21
Abundance worms > 1 cm (worms/m²)	8 090	8 180	9 640	8 700	8 650 ± 710
Abundance worms > 5 mm, < 1 cm (worms/m²)	7 450	6 630	8 650	7 700	7 610 ± 830
Abundance worms < 5 mm (worms/m²)	2 370	2 710	1 210	2 450	2 180 ± 670
Overall worm abundance (worms/m²)	17 910	17 520	19 500	18 860	18 500 ± 500

counting (worms retained on a 2-mm sieve are highly visible). During this analysis, oligochaetes were classified into three size categories: worms greater than 1 cm, worms 5 mm to 1 cm, and worms smaller than 5 mm. Samples were retrieved in late January of 2002. Table 3.2 shows results for the more detailed analysis.

3.2.3 Taxonomic Classification

Although some species of chironomids (larvae) and copepods were seen in the samples, abundances were low and the species were thought not to be significant contributors to the bioturbation potential in South Lake. As mentioned before, the bulk of organisms collected were oligochaete worms. Upon careful inspection under low-powered microscopes, three distinct types of worms were identified. Although genus and species were not determined due to a lack of expertise, all three worm types were determined to be

of the family Tubificidae. This is due to the presence of setal bundles beginning on the second body segment (from the head end), the lack of any eyes or prominent proboscis, and sizes ranging from approximately 1 mm to well over 20 mm and less than 1 mm in diameter. The least abundant and largest of the three worm types is believed to belong to the genus *Branchiura* due to the presence of dorsal and ventral gills near the posterior end of the worm (Smith, 2001).

According to Smith (2001), tubificid worms, an order of Annelid worms similar to the common earthworm, feed on deposits, filamentous algae, diatoms, or plant and animal detritus. These worms are typically head-down, conveyer belt deposit feeders. The term conveyer belt is used due to feeding patterns in which sediment particles are ingested at depth (the “feeding depth”) and egested on the surface as feces. Robbins *et. al.* (1979) showed that radioactive material at the sediment-water interface resulted in wide peaks and well-diffused activity profiles after periods of only 60 days in the presence of tubificid worms. Swift (1993) ranked species’ contribution to the bioturbation process according to certain mobility, feeding, and burrowing patterns. Although only limited free movement is possible for oligochaetes and burrowing activities are not observed, these conveyer belt species contribute largely to the bioturbation process through feeding activities (overall rank is 5 or 6 on a scale of 1–11, 11 being the highest potential and 1 the lowest).

3.3 Bayou Braud

Bayou Braud is located on the south end of the Cypress Flats swamp, just below Alligator Bayou in Ascension Parish (see Figure 3.2). Bayou Braud is a 2 km long channel with average center depth of around 1 m and approximate width of around 30 m. The soft sediment layer is fairly deep and the overlying water is virtually calm. Unfortunately, it was

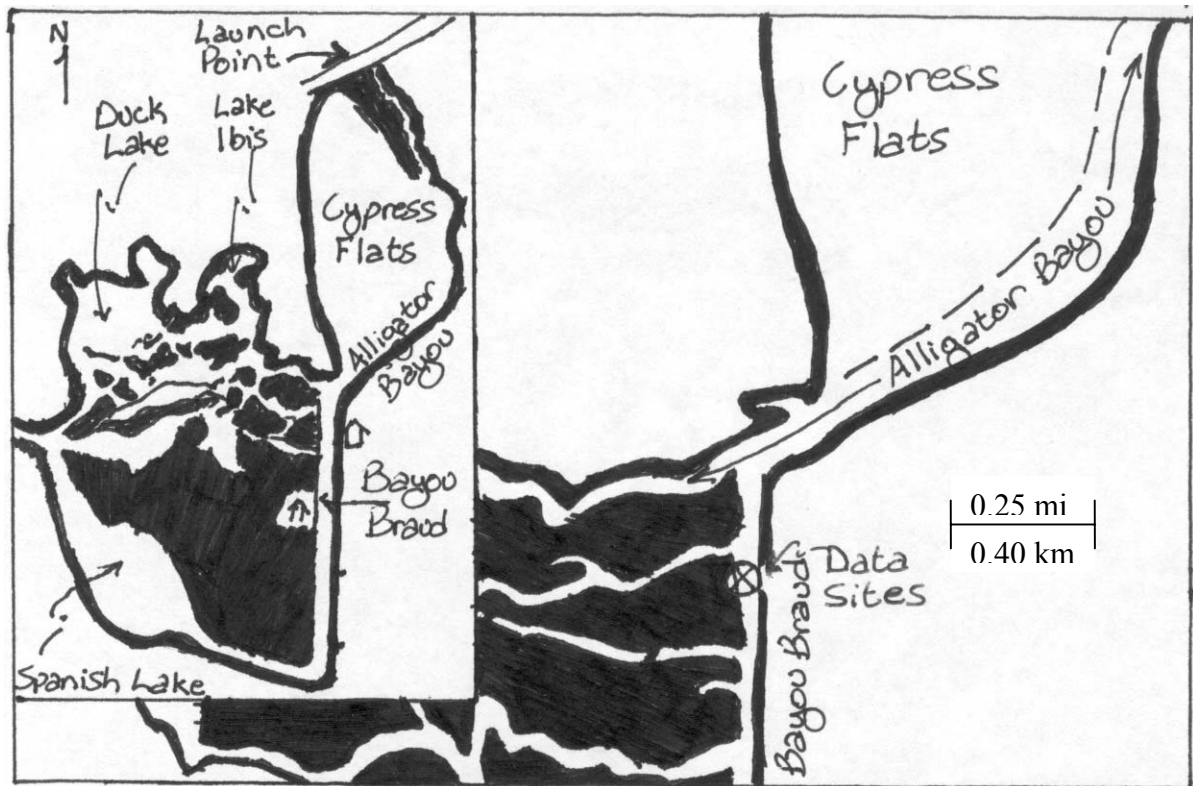


Figure 3.2 Details of Bayou Braud Site

later discovered that there is a relatively large amount of boat traffic on Bayou Braud because of its convenient access to Spanish Lake, a popular duck hunting location.

Table 3.3 Detailed Benthic Analysis of Bayou Braud (December, 2001)

Sample	Sample
Count large worms (> 1 cm)	242
Count medium worms (> 5mm, < 1 cm)	191
Count small worms (< 5 mm)	248
Total Count	681
Abundance worms > 1 cm	2 600
Abundance worms > 5 mm, < 1 cm (worms/m ²)	2 060
Abundance worms < 5 mm (worms/m ²)	2 670
Overall Organism Abundance (worms/m²)	7 330

A preliminary benthic analysis showed that Bayou Braud has a well-established benthic community. A more detailed analysis, similar to the one conducted in Capitol Lake, but using a sample area approximately four times greater, confirmed this and the results are

shown in Table 3.3. Most significant bioturbators are again species of tubificid oligochaetes, indicating that the dominant mode of transport in the Bayou sediment is a conveyor belt mechanism. Based on these site characterizations, we believed initially that Bayou Braud would be a good site for performing research.

Despite favorable sediment conditions in Bayou Braud, three attempts to obtain data were unsuccessful. In November of 2001, the pole marking the location of our sample plot was missing, perhaps removed by one of the many boaters passing through the area. Also, an alligator had apparently established its nest in this spot, preventing us from collecting data from the approximate location in which we set the plot. Future plots were set up with multiple markers, both exposed and submerged, to prevent future recurrence. Later that month a new sample plot was laid out, but cores collected during December of 2001 from the new plot were strongly depleted of magnetite, leading us to the conclusion that magnetite was not reaching the bottom. Then, a third plot was laid in late December. Initial cores taken from this third plot were analyzed and the results confirmed that very little magnetite was reaching the sediment surface. We believe this is due to the large amount of submerged aquatic vegetation present in the sample area. Attempts to sample from these plots were often thwarted by large systems of plant roots interfering with core retrieval. Often, these plants trapped gas bubbles beneath their leaves and stems. Then, magnetite falling through the water column would agglomerate around these gas pockets and not fall to the sediment surface, as evidenced by the surfacing of magnetite-covered gas bubbles nearly an hour after the sample plot had been prepared. Because of the many difficulties experienced while attempting to develop this site, it was abandoned in order to focus efforts on the more productive Capitol Lake site.

Chapter 4

Experimental Design and Procedures

4.1 Overview

As mentioned in Chapter 1, the objective of this research was to develop and test a routine, *in situ* technique for measurements of sediment biodiffusion coefficients in aquatic sediments that can detect seasonal or other time period variations. In accomplishing this goal, magnetite, an iron oxide that is magnetic, inexpensive, nontoxic, and readily available, was chosen as a sediment particle tracer. Ideally, such a technique would disperse the tracer into a thin and uniform layer entirely on the surface of the sediment. Then, the progress of the magnetite particles could be checked at later time intervals by coring the mud, and magnetite concentration profiles could be analyzed to estimate biodiffusion coefficients. The following sections describe the procedures for establishing sample plots, sampling from the plots, preparing the retrieved samples, and analyzing the prepared samples. The final section gives details of a laboratory experiment conducted to determine whether or not the oligochaetes selectively ingest or reject the magnetite particles applied to the sediment.

4.2 Sediment Tracer Experiments

The bulk of this research consists of *in situ* tracer studies in the sediment of Capitol Lake. These studies encompass establishment of data plots, sampling of experimental plots, preparation of retrieved samples, and analysis of prepared samples. Calculation of biodiffusion coefficients will be discussed in Chapter 5 as a part of the discussion of results section.

4.2.1 Establishment of Research Plots

Access to research plots was accomplished using a small boat. The boat itself was a small Johnboat, 3.6 m in length and 1.4 m wide. The front and rear of the boat were fitted with 5.4 kg anchors to keep the boat from drifting, and propulsion was accomplished with oars. The marking poles used in the experiments were 2.6 m plastic tomato stakes.

Magnetite is in crushed form and particles coarser than 600 μm are separated by sieve and discarded. Table 4.1 contains physical properties of magnetite and Table 4.2 gives the particle size distribution for the magnetite used in this research. Magnetite in crushed form was obtained from Leslie Ceramics Supply, 1212 San Pablo Ave., Berkeley, CA 94706, (510) 524-7363.

Table 4.1 Physical Properties of Magnetite

CAS Number	1317-61-9
Chemical Formula	Fe_3O_4
Decomposition point	1538°C
Molecular Weight	231.55 g/mol
Specific Gravity	5.18
Water solubility	Insoluble

Table 4.2 Particle Size Distribution of Magnetite Used in Tracer Experiments

Size Range (μm)	Weight Fraction
25-74	0.045
74-125	0.099
125-200	0.300
200-250	0.211
250-300	0.113
300-425	0.092
425-500	0.049
500-600	0.090
Weighted Average Particle Diameter	245 μm

Before preparing the sample plots, an adequate spot in the lake must first be selected as defined by ease of sampling, amount of organic debris in sediment (such as leaves and sticks), and depth of the overlying water column. Sediments from near the chosen location are examined, and, if acceptable, the plot is established. In setting up the plot, the boat is first anchored on each end by casting out an anchor and pulling them taut. Then, a marking pole is placed in the sediment deep enough to secure it in the sediment, but with the top visible above the air-water interface. Next, approximately three pounds of magnetite are sifted over the water directly above the sample plot, an area approximately 1 m in diameter. This is carried out with a 600 μm (no. 30) sieve to prevent particles larger than the diameter of the benthic organisms in the sediment from sinking into the plot and causing misleading results. Because magnetite tends to float on the water, it is necessary to break the surface tension by slight agitation with a stick or by hand after sifting enough to lightly coat the surface of the sample plot. After all magnetite has been deployed, initial core samples are taken from the plot (see section 4.2.2 for core sampling procedures) for analysis to ensure that magnetite has adequately covered the sample area.

4.2.2 Sampling Procedures

In order to get an accurate account of the effects of bioturbation over the course of the experiment, it is necessary to obtain nearly flat, undisturbed samples of the sediment layers. The sampler used is shown in Figure 4.1. Essentially, empty sample core tubes, each approximately 5 cm in diameter, are extended by clamping them to one end of a 2-m hollow PVC conduit. This allows the sample tube to be pushed into the sediment by a person sitting in the boat. Holes are drilled through the conduit at regular intervals to allow is also fitted with a suction piston to keep sediments from sliding back out of the end of

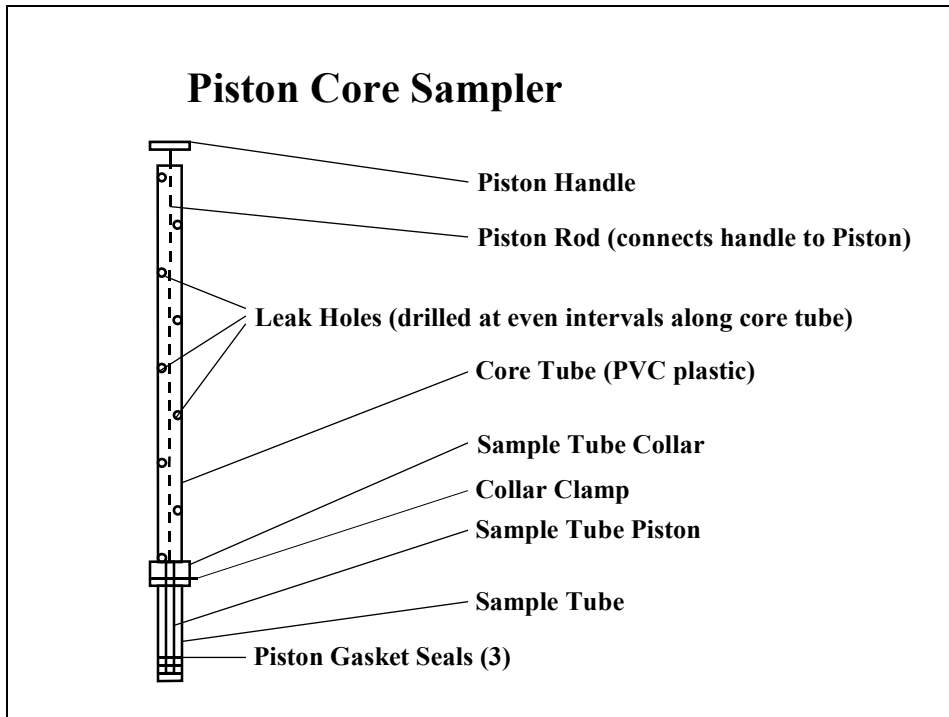


Figure 4.1 Piston Core Sampler Diagram

the sample tube once removed from the lake bottom. The piston is controlled separately from the sample tube by a rod going through the hollow center of the conduit and attached to a handle. Three gaskets between the piston and the sample tube wall seal pressure into the sample tube. Once the sample is retrieved, the ends of the sample tube are readily sealed using plastic caps slightly larger in diameter than the sample tube. Retrieved samples are transported in a vertical position using a sample tube holder to prevent them from tipping over and disturbing the horizontal sediment layers.

To assemble the coring apparatus for sampling, the piston gaskets are first lubricated with petroleum jelly. Then, the piston is pushed through the entire length of the sample tube and back again to lubricate and create a seal and eliminate excess friction. The piston bottom is then moved to approximately 1 cm from the bottom edge of the sample tube. This prevents the weight of the coring apparatus from smearing the top sediment layer upon

reaching the lake bottom. Next, the piston is attached to the piston rod through the eyebolt mounted on top of the piston. The sample tube and piston are then pushed into the collar connecting to the PVC conduit and the clamp is tightened with a screwdriver to secure the sample tube.

Sampling is accomplished by lowering the sample tube end of the assembled apparatus through the water column slowly enough to allow water to enter the conduit and equalize the pressure within. Once the tube reaches the bottom, the tube is pressed firmly into sediment while the handle attached to the piston rod is held steady to keep the piston positioned just above the sediment surface. Once the piston reaches the top of the sample tube, as evidenced by resistance to further movement through the tube, the entire apparatus is lifted gently out of the sediment. Before removing the core from the water, it should be gently cleaned away from the sample plot to remove sediments clinging to the exterior of the tube. This will keep sediments from settling on top of the data plot and tainting the results. Once cleaned, the core should be removed from the water and a cap placed over the bottom of the sample tube. Then, the tube is removed from the core apparatus by loosening the collar clamp with a screwdriver and disconnecting the piston rod from the eyebolt on the top of the piston. Finally, the piston is removed from the sample tube by compressing the gasket against the tube wall to break the seal and thereby allow easy extraction from the tube. A second cap is then placed on top of the sample tube and the closed tube is stored upright in a sample tube holder.

When samples are brought to the surface, it is important to examine the top layer. If the surface of the sediment is uneven (with distances greater than 2 mm from the highest peak to lowest valley) or is otherwise flawed, it becomes necessary to discard the sample

and retrieve another core. Once all cores have been retrieved from the sample plot, cores are transported back to the laboratory for analysis. Within two hours of extraction from the lake, retrieved data cores are treated with 5–6 drops of 10% buffered formalin to prevent bioturbation to continue.

4.2.3 Core Extrusion and Slicing

Before obtaining data from retrieved core samples, it is necessary to section the core into slices of equal thickness. A diagram of the piston-type extruder used is shown in Figure 4.2. This device consists of a support arm with a screw clamp to push spacers into the tube mounted to a counterweighted base for stability. Full sample tubes are mounted to the support arm by tightening the two support clamps around the tube with a screwdriver, being sure to mount the tube high enough to maneuver spacers and the adjustable screw clamp below the tube. As the bottom cap is removed from the sample tube, a piston, identical to the small gasketed section of the piston on the core sampler, is positioned at the bottom of the sediment sample and carefully pushed into the tube, forcing the entire core upwards. Next, large spacers, each 19 mm thick, are pushed into the tube until the top of the sediment is less than one large spacer's thickness from the top edge. Then, small spacers, each 1.58 mm thick, are added one at a time to the base plate and pushed up until the top edge of the sediment is approximately flush with the top of the sample tube. At this point the sediment is ready for slicing. This is accomplished by extruding the sediment out the end of the sample tube and slicing the top at regular intervals. The wet sediment slices are then dried for 24 hours in an oven at 105°C to prepare them for final data analysis.

Actual slicing of the core requires repetition of various steps for slicing each section. First, a small spacer (1.58 mm diameter) is added to the base plate and pushed up by raising

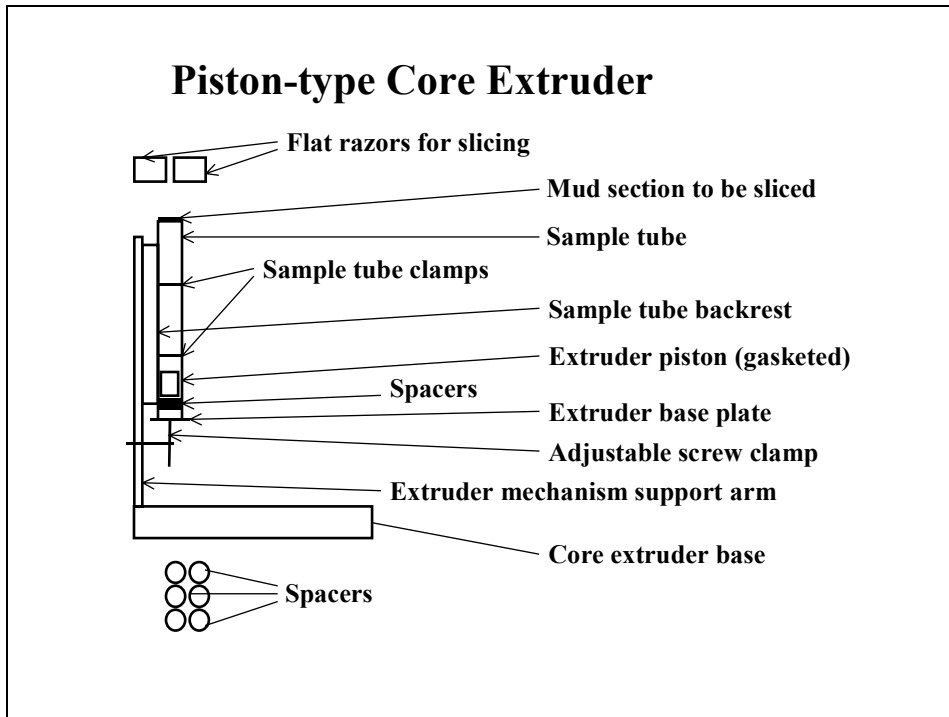


Figure 4.2 Piston-Type Extruder Diagram

the screw clamp to push against the plate and turning it until the plate is firmly pressed against the bottom of the sample tube. Then, the two razors are used to slice the sediment by starting at either edge and slicing toward the center of the core, following the tube edge as a guide. The slice is then removed from the sediment sample by carefully sliding the razors off of the top of the sample tube. Sliced sediment is then thoroughly scraped from the razors into a clean aluminum sample dish, appropriately labeled with the core identification name and slice number. Once all slices have been collected, fifteen per core for this research, the remainder of the core is discarded and the sample tube is cleaned. All sample trays are transferred to the oven for drying overnight.

4.2.4 Analysis of Core Sections

Because we desire to obtain tracer concentration-depth profiles, magnetite must be separated from each sample slice and weighed. Each slice is the same thickness and diameter, and concentrations can be calculated straightforwardly as mass over volume. Analysis is carried out in a letter-sized tray approximately 23 cm x 30 cm x 5 cm high. Separation is accomplished with a 1.3 cm diameter, 1.3 cm high rare earth magnet with a maximum of 10 lbs of pull. The magnet is fitted with a paraffin and paper sheath to ease removal of magnetite from the magnet. Before beginning, dried samples should be removed from the oven. A clean paper liner is placed in the analysis tray and a second liner is laid beside the tray for purifying recovered magnetite. The magnet should be fitted with a new sheath and a fresh piece of soft tissue paper for sample purification obtained. Finally, the sample tray and all components should be inspected carefully and cleaned, if necessary, to ensure that no magnetite is present initially on the equipment.

Before separation of magnetite from the sediment is possible, the dried sample must be ground in a mortar and pestle. Next, a brush is used to clean the sides of the mortar and the powdered sediment is sprinkled through a sieve onto the sample liner in order to catch any coarse lumps of sediment. The coarse lumps are then ground in the mortar again and mixed with the rest of the sample on the liner. Being certain to cover the bottom of the magnet with a paraffin and paper sheath, paper side out, the magnet is slowly swept back and forth just above the surface of the liner in order to draw the particles upward from the remaining sediment. Once the entire tray has been swept free of magnetite particles, the magnet is moved to the other liner and the magnetite particles released by pulling the magnet from the sheath while the separated particles fall on the liner. These particles are

then rubbed very gently with a soft tissue to further loosen and separate agglomerated sediment from the surface of the magnetite. This magnetite is then transferred to a weighing dish and weighed using a Mettler electronic balance. Weights are recorded in grams to three significant figures. This procedure is repeated for each of the remaining samples.

4.3 Fecal Matter Collection Experiments

The purpose of these experiments was to test the ingestion characteristics of oligochaete worms and determine if they select or avoid the magnetite particles in the sediment. Although tracer motion through the sediment due to bioturbation is not solely dependent upon the principle bioturbating species non-selectively ingesting magnetite particles with sediment, its importance may lie in long-term studies and in studies involving rapidly mixed depth, usually the top ½ to 1 cm in the sediment. To create the materials used in this experiment, 400 mL of sediment from Capitol Lake was mixed homogeneously with approximately 10 grams of magnetite. The experimental apparatus follows the setup used by Lotufo and Fleeger (1996) for similar experiments (See Figure 4.3).

Setting up the experiment involves filling a 2.5 cm diameter, 50-cm³ centrifuge vial approximately two-thirds full of the magnetite-spiked sediment. To this is added 10 mL of artificial pond water, which consists of water enriched with various nutrients (see Table 4.1). This is allowed to equilibrate for roughly 6 hours in an incubator at 26°C. Once the system has been acclimated to the pond water, excess water is decanted with a pipette and the tube is inoculated with twenty oligochaete worms of the species *Ilyodrilus templetoni*, each approximately 1 to 2 cm in length. Once the worms have tunneled into the sediment, the surface is covered with a thin layer of polyester floss and a disc of cheesecloth. These are

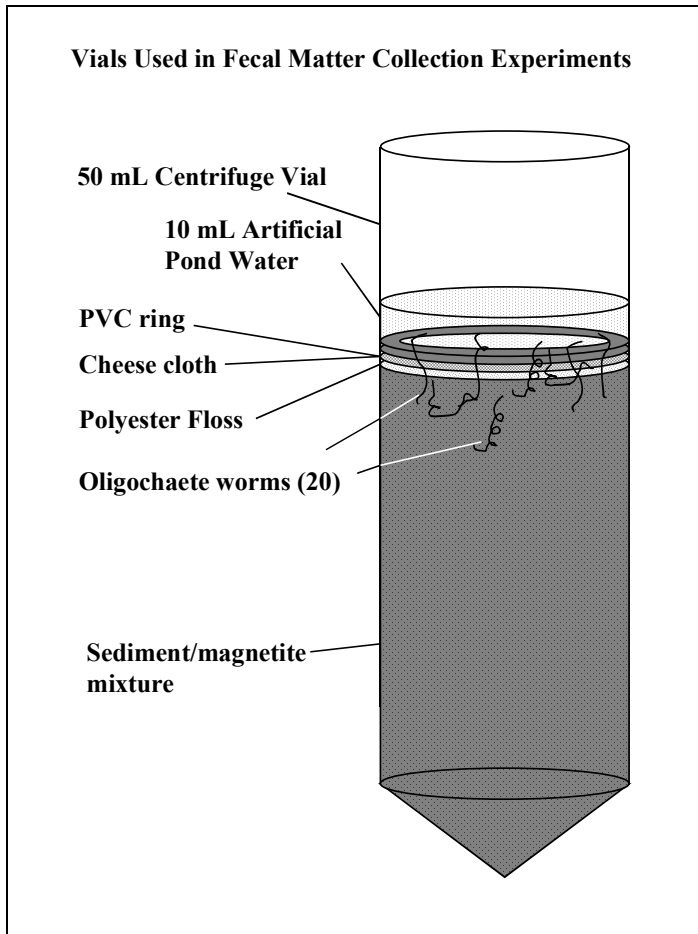


Figure 4.3 Oligochaete Fecal Matter Collection Experiment Apparatus

held in place by a PVC ring around the edges of the tube. Finally, fresh artificial pond water is added to the sample and the vial is returned to the incubator. The artificial pond water must be decanted and refreshed on a regular basis to maintain the organisms' health in the sediment.

Table 4.3 Nutrient Concentrations in Artificial Pond Water (APW)

Chemical	Concentration	Chemical	Concentration
NaCl	0.5 mM	KCl	0.05 mM
NaHCO ₃	0.2 mM	CaCl ₂	0.4 mM

Every 24–48 hours or when possible, feces was collected from the surface of the cheesecloth. This is accomplished by siphoning the feces via pipette from the cloth surface

and placing them in an aluminum sample dish. Artificial pond water levels were replenished at this time, as well. Next, fecal samples were dried in the oven at 105°C and then analyzed as described in section 4.2.4. Separately, concentrations of the original magnetite-laden sediment are dried, weighed, and analyzed to determine the preference, if any, of oligochaetes for or against ingesting magnetite. Comparison of the magnetite concentrations in fecal matter with that in the bulk sediment will give information on selectivity.

Chapter 5

Presentation and Discussion of Results

5.1 Overview

The intent of this research was to develop a chemical-particle tracer protocol that can be used for measuring biodiffusion coefficients in short time intervals. After several unsuccessful experiments were conducted, the refined methods for tracer broadcasting, sample retrieval, and data analysis (discussed in section 4.2) were designed and implemented. This chapter will first look at the outcome of the fecal matter collection experiment for selectivity determination. Then, the remainder of the chapter will be dedicated to presenting and discussing the results of three experiments conducted on Capitol Lake in late 2001 and early 2002. First, representative raw data will be presented and discussed. Next, a numerical model for interpreting the data will be presented, and methods for data analysis will be outlined. Results from the three experiments will then be presented and compared with results from similar experiments in the literature.

5.2 Fecal Matter Collection Experiments

A fecal matter collection experiment was conducted in the laboratory as detailed in section 4.3. At intervals of approximately 48–72 hours, fecal matter samples were collected from the experimental apparatus and dried. The dried sediment was then analyzed to determine the amount of magnetite present in the feces of the oligochaetes. This concentration was then compared to the concentration of the magnetite in the bulk sediment, as determined by the composite result of six individual sample analyses. Table 5.1 shows the results of these analyses.

Table 5.1 Results from Fecal Matter Collection Experiments

Sample	Concentration in sample (g magnetite/g dry sediment)	Sample to standard concentration ratio
Standard (bulk sediment)	0.0402 ± .0020*	1.000
Fecal Matter Sample 1	0.0174	0.4337
Fecal Matter Sample 2	0.0262	0.6520
Fecal Matter Sample 3	0.0177	0.4397
Fecal Matter Sample 4	0.0334	0.8312

*based on a composite result from six samples of bulk sediment

The first data column of the table is the concentration of magnetite in each sample, measured on a weight basis with the dry sediment. The second data column gives a ratio of the sample concentration to that of the bulk sediment, a convenient statistic for establishing whether or not the oligochaetes are selectively feeding on magnetite. Although a wide variation is observed in the sample:standard ratios calculated, some degree of selectivity against magnetite and in favor of the sediment seems to be occurring. This is likely due to larger magnetite particles being present in the sediment that the oligochaetes are incapable of ingesting. Another possibility that exists is that, despite careful sampling and handling procedures during experiments, bulk sediment laden with magnetite could potentially have been siphoned through the floss and cheesecloth layers, giving the faulty appearance of a high magnetite concentration in the feces. Some variability could be caused by existence of pockets in the sediment that contain very little magnetite compared to the bulk.

One important thing to consider is that the lack of selectivity is not absolutely necessary for the tracer to accurately model the short-term effects of bioturbation. The tracer, which is unable to reach the feeding depth over the course of the experiment, will still have a net downward motion resulting from feces deposited on the surface and thus moving the subsurface layers downwards. This effect occurs regardless of the feeding preferences of the bioturbating species. The average feeding depth of the oligochaetes is approximately

equal to their average body length of 1.5 cm. Experiments that allow the tracer enough time to reach the feeding depth, however, may result in inaccurate final results due to the tracer not properly being transported back to the surface. Because most of our tracer is confined to the upper two centimeters of sediment after a one month period, it is believed that selectivity has little effect on the overall usefulness of magnetite as a tracer in our experiments.

5.3 Presentation of Raw Data from Tracer Experiments

The following sections will outline the results and interpretations of three separate tracer experiments conducted during December 2001, January 2002, and February 2002, respectively. First, the calculated loadings for each core will be compared and discussed to indicate the effectiveness of the broadcasting technique. Next data will be presented and the analysis process will be detailed. Each experiment was conducted over a period of approximately 30 days, at the end of which five replicate samples, labeled Cores 'A' through 'E', were retrieved for analysis. While all data graphs are included in the appendix, only three representative sample analyses will be presented in this chapter. This should provide sufficient examples to adequately describe the protocol outcomes without being burdened by extraneous and cumbersome graphs.

Table 5.2 shows the values of tracer loadings found in each replicate. Originally, enough magnetite was broadcast over an area approximately 1 m in diameter so that a uniform weight of approximately 3 g per core would result. Actual values retrieved were often far lower, indicating that only a fraction of magnetite broadcast at the surface settled onto the targeted area. Because of the particle diameters (245 μm) and high specific gravity (5.18), it is unlikely that tracer was washed away due to resuspension. Water depth at the site was approximately 2 m. Some improvements to the broadcasting technique, especially

Table 5.2 Tracer Loadings for Experiments Conducted on Capitol Lake

Core Number	Magnetite Loading, g/core		
	Experiment 1	Experiment 2	Experiment 3
Core ‘A’	0.388	0.744	0.311
Core ‘B’	1.723	0.156	1.174
Core ‘C’	1.015	0.513	1.310
Core ‘D’	0.843	0.278	0.424
Core ‘E’	0.823	0.711	0.485

those involving placement of prepared cores into the lake sediment via scuba divers, would certainly improve the consistency and uniformity of tracer delivery onto the sediment surface.

Examples of three magnetite particle weight-depth profiles are shown in Figures 5.1, 5.2, and 5.3. While all three figures demonstrate a diffusive characteristic profile, these were chosen specifically to illustrate the types of desirable and undesirable profiles possible depending on environmental factors. The first two graphs, depicting core ‘C’ from experiment 2 and core ‘B’ from experiment 3, have high tracer loadings at the surface that taper off dramatically within the top centimeter of sediment. This is followed by a long section of low tracer loadings, generally referred to as the “tail”. The reason this tail is observed may be the result of artifacts arising from drawdown during coring and extruding, and/or due to non-diffusive sedimentation into pore spaces during. Because these loadings are almost certainly due to events other than biological mixing activities, the tail section is ignored during final modeling; in addition, it has been found to have little impact on final results.

The third core, core ‘C’ from experiment 1, is characterized by two large subsurface peaks with only a small surface concentration, comparatively, and no apparent tail. Upon extrusion, it was found that this core exhibited several undesirable characteristics. First,

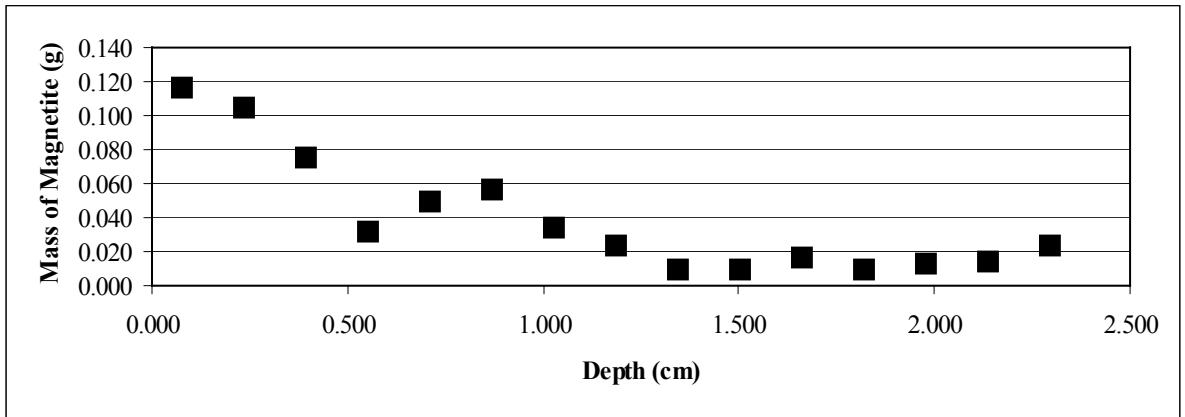


Figure 5.1 Tracer Weight-Depth Profiles from January 2002, Core 'C'

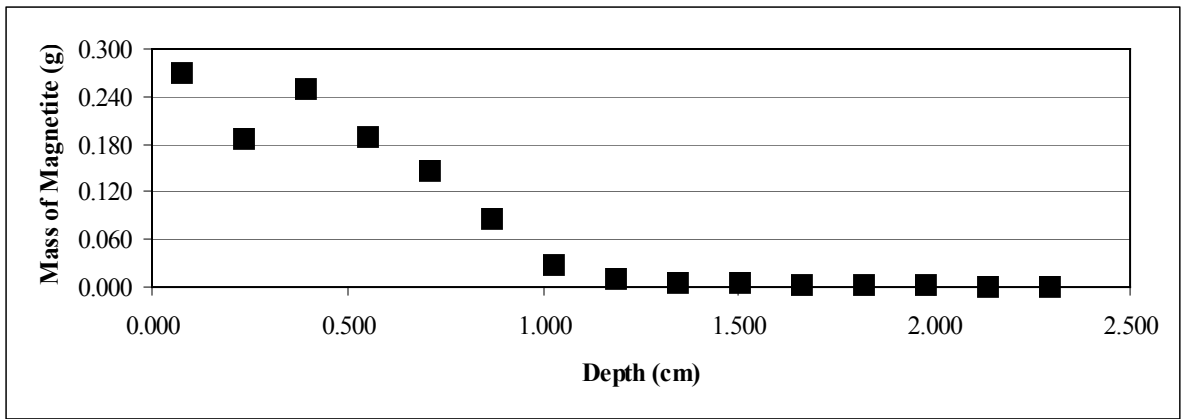


Figure 5.2 Tracer Weight-Depth Profiles from February 2002, Core 'B'

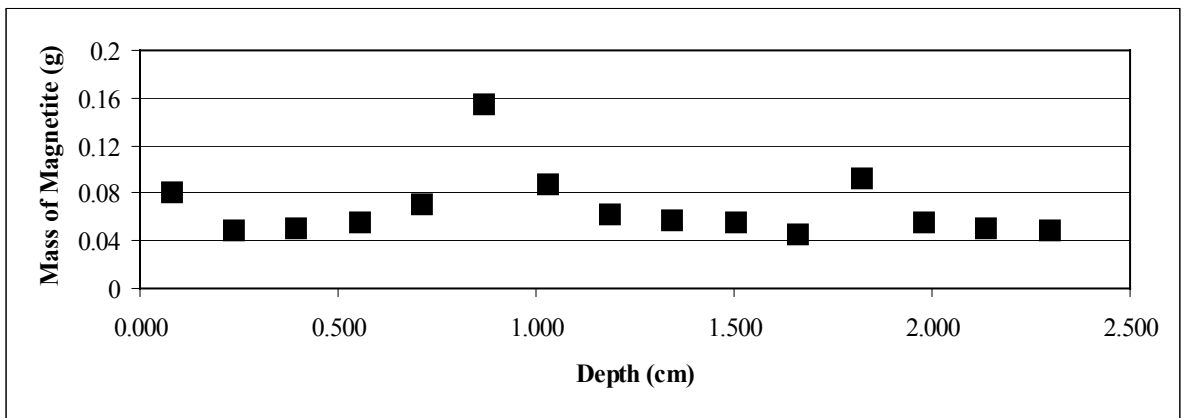


Figure 5.3 Tracer Weight-Depth Profiles from December 2001, Core 'C'

many shallow impressions marred the surface leading to higher loadings in the subsurface slices near the top. Secondly, a nearly 13% grade of the surface made accurate top slicing difficult—a flat sediment surface topography in the core is necessary for good results. The high loadings present as far as 2 cm into the sediment are possibly due to magnetite accumulating in a depression in the sediment surface. This depression may have been caused by an animal (such as a crawfish plowing through the sediment) or by plant debris (such as a tree limb falling on the sample surface), although other sources are certainly possible.

Several sediment conditions must exist in order for the successful retrieval of good, representative data samples to be possible. Of course, any results are dependent upon the existence of a well-established benthic organism population with an adequate number density in the sample plot. A minimal amount of air pockets and plant debris, which interfere with results, is also desirable. Equally crucial is a sufficient tracer mass loading to accurately track sediment processes through the upper sediment layers. Above all, good results can only occur when retrieved samples have flat surfaces unmarred by depressions. Many of these factors can be identified by taking preliminary samples and examining them prior to establishing new sample plots. However, as is obvious when examining core ‘C’ from December 2001, bad analysis results are still possible, even after careful preparation. Also, some degree of noise will always be present in the data due to the widely varying conditions found in the sediments and inconsistency in magnetite deployment.

5.4 Data Analysis

5.4.1 Model Description

As mentioned in section 2.3, the simplified, unsteady-state diffusion model without sedimentation term (equation 2.11) is used for data analysis in this research:

$$\frac{\partial C}{\partial t} = D_b \frac{\partial^2 C}{\partial z^2} \quad (2.11)$$

This model has the following solution, given by Crank (1976):

$$C(z, t) = \frac{M}{\sqrt{\pi D_b t}} \exp\left(\frac{-z^2}{4D_b t}\right) \quad (5.1)$$

where: M = tracer loading per unit area, g/cm^2

D_b = biodiffusion coefficient, cm^2/yr

t = time, yrs

z = depth in sediment, cm

This solution is for diffusion processes into a semi-infinite slab over a time period of t years. The initial condition used in obtaining this solution is a Dirac delta function ($\delta(z-z_0)$), which has the properties of an infinitely thin layer of tracer input entirely at the sediment surface ($c = 0$ at $t = 0$, $z > 0$). Concentration is assumed 0 at infinite depth for all $t \geq 0$, and the total loading, M , is assumed constant over the course of the experiment (no lateral or nonlocal exchange occurring).

5.4.2 Initial Sample Profiles

One assumption made in obtaining the solution for the model given in equation 5.1 is that the entire tracer inventory is found on the surface of the sediment immediately after deployment. However, analysis of several cores taken at times just after tracer broadcasting ($t \approx 1$ hr, the average time elapsed between sample coring and addition of biocide to sample

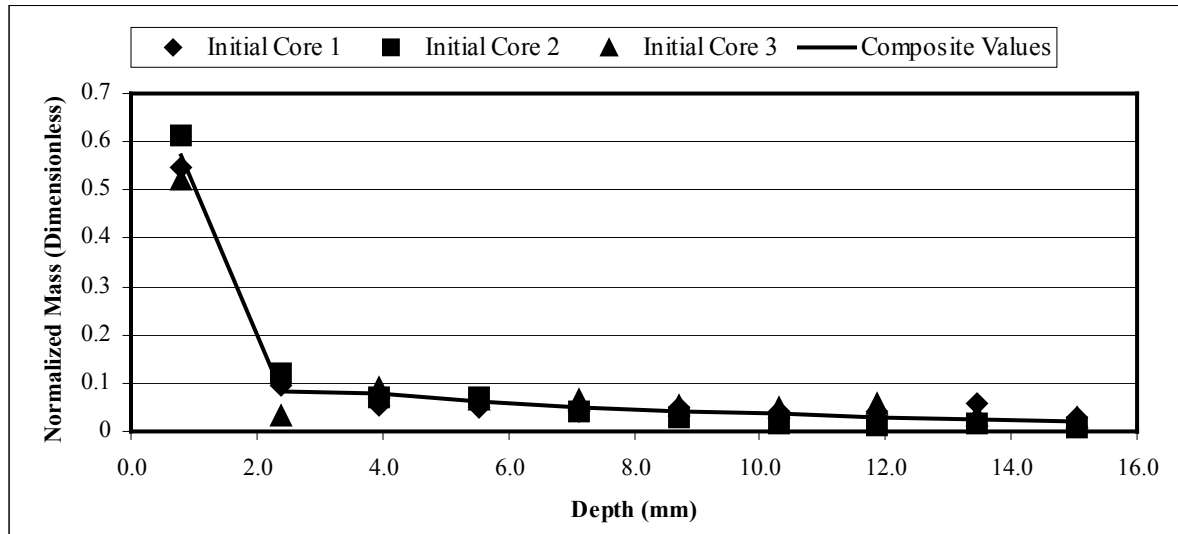


Figure 5.4 Normalized Initial Tracer Profiles for Capitol Lake

cores) reveals that an initial profile exists (see figure 5.4). Fitting these profiles to the model solution using non-linear regression (see curve fitting procedures in section 5.4.3) gives values for $D_b \approx 20\text{--}30 \text{ cm}^2/\text{yr}$, which are much higher (two orders of magnitude) than expected from the sediment. Fornes *et. al.* (1999) observed similar initial depth distributions in continental slope sediment and attributed them to passive deposition into tubes and burrows created by benthic organisms. In the case of magnetite with a specific gravity of 5.18, the penetration may be gravity settling and displacement of the less dense sediment grains with specific gravities of 2.0–2.6. Because of the unreasonably high D_b values over the short time periods of initial cores retrieved, passive deposition is believed to be a substantial factor in the raw data profiles observed, and therefore must be corrected to avoid calculating highly inflated final values of D_b .

Because initial profiles taken from three different spots in Capitol Lake do not vary appreciably, the initial depth distribution of magnetite is taken to be constant with respect to

position in the lake. Three profiles from initial samples, each normalized by dividing the mass in a given slice by the total mass in the sample, are plotted in figure 5.4. The composite profile (shown as a line on the figure) can be used to transform data by subtracting initial values of normalized mass in layers below the surface to account for background loadings or sampling artifacts. Correcting data in this fashion shows the actual progression of tracer diffusion due to bioturbation

5.4.3 Curve Fitting Procedures

Curve fitting is accomplished using a nonlinear regression analysis algorithm available in a spreadsheet program. For this research, Microsoft Excel™ is used because of the powerful iterative equation solver (“solver”) built into the software package. Two parameters are regressed: the biodiffusion coefficient, D_b , and the actual position of the sediment-water interface, modified by a depth adjustment parameter, z_0 . The latter parameter is considered an unknown because the point observed to be the top of the core could actually contain a thin layer of material deposited on top of the surface from materials suspended in the water column. Also, since the slicing interval is finite and does not always align the top of the sample tube with the sediment surface during slicing, the position of the interface within the first slice is not necessarily at the top of the slice. Furthermore, because the sedimentation term of the model is neglected, any small amount of bed consolidation due to the dense magnetite particles on the surface can be accounted for with this term as well.

Concentration profiles must be derived from the raw data. First, loadings are normalized by dividing them by the total mass of tracer in the sample. These loadings are then corrected for the presence of an initial profile (as shown in figure 5.4), according to the method given in section 5.4.2. The final corrected tracer weight-depth profile is converted

to a concentration-depth profile by dividing each data point by the volume of a slice, since each section has the same thickness and cross-sectional area. Then, before regressing the data, the “tail” of the data is truncated so as to consider only the significant points in the analysis. Although no absolute rule exists for defining the tail, it is generally chosen as the third and higher depths at which the normalized concentration is close to 0. Because the concentrations have been normalized, the mass loading, M , must also be normalized as:

$$M^* = \frac{M}{m} \quad (5.2)$$

where: M^* = normalized mass loading, cm^{-2}

M = mass loading, g/cm^2

m = total tracer mass in sample, g

From this relation and equation 5.1, the normalized concentration distribution is found to be the following:

$$C_i^* = \frac{M^*}{\sqrt{\pi D_b t}} \exp\left[\frac{-z_i^2}{4D_b t}\right] \quad (5.3)$$

where: C_i^* = normalized concentration at depth

Figures 5.5, 5.6, and 5.7 show the data from figures 5.1, 5.2, and 5.3 converted to normalized concentration profiles. The presence of above-background concentrations in the layers below the top indicate that some degree of diffusive mixing has taken place. Also, because the solution is exponentially decreasing with the square of the depth, only the first few data points have a large bearing on the final value of D_b . The last graph has negative values in the second, third, and fourth positions, an occurrence that is not physically realizable, and thus forces the biodiffusion coefficient to be very small. This is most

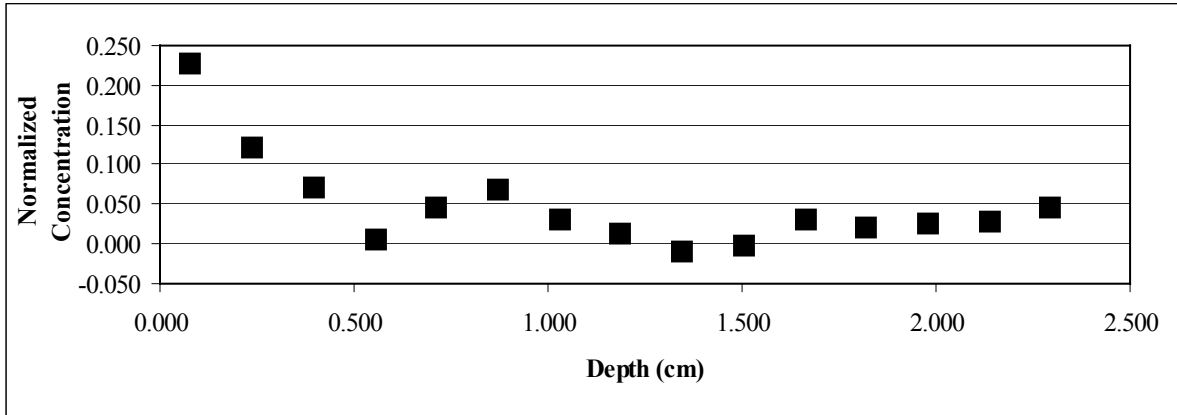


Figure 5.5 Normalized Concentration-Depth Profiles, Core 'C' From Experiment 2

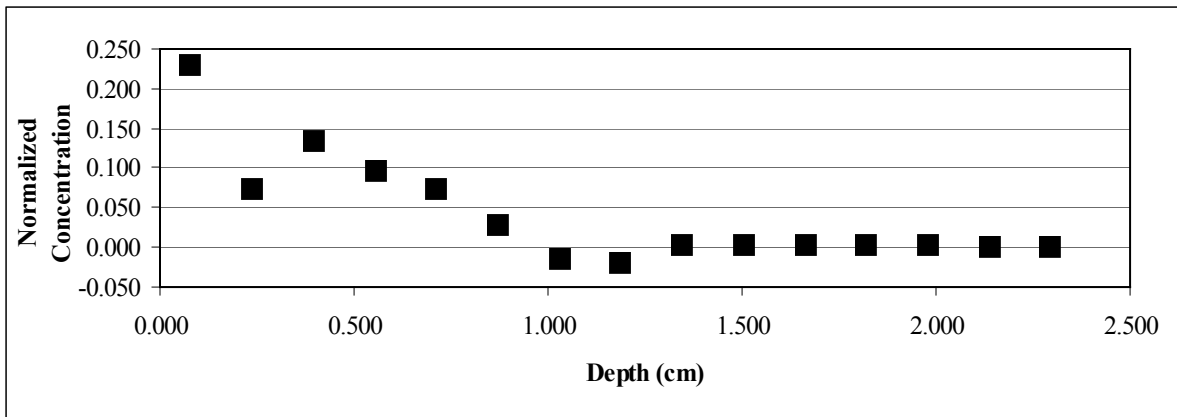


Figure 5.6 Normalized Concentration-Depth Profiles, Core 'B' From Experiment 3

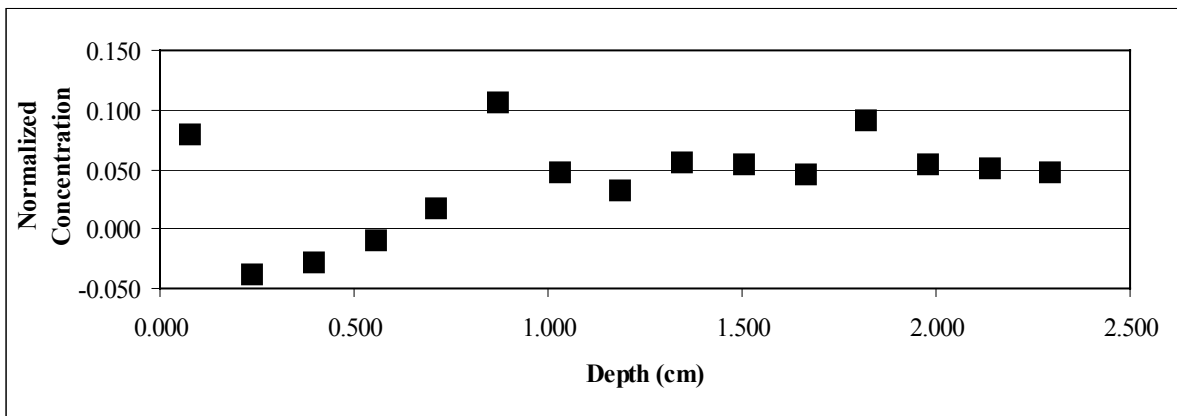


Figure 5.7 Normalized Concentration-Depth Profiles, Core 'C' From Experiment 1

probably a result of using average initial weight-depth profiles when, in fact, it is inappropriate for specific cores with low initial loadings. Also, the irregular surface topography and grading may result in a non-conforming initial profile.

Actual curve fitting of the data is accomplished using the software package to find values of the biodiffusion coefficient, D_b , and of the location of the sediment-water interface as given by a depth adjustment parameter, z_0 , such that:

$$z_i = z_{i,\text{meas}} + z_0 \quad (5.4)$$

where: z_i = actual depth of data point, cm

$z_{i,\text{meas}}$ = observed depth of data point, cm

z_0 = depth adjustment to account for interface position.

Figure 5.8 shows an example setup for fitting parameters to the model for core ‘C’ from experiment 2. The top two rows contain values for the biodiffusion coefficients and depth adjustment parameter. These are each given initial guesses based on expected final values before invoking the equation solver. The leftmost column shows the depths within the core adjusted by the value of the depth adjustment parameter. The adjacent column gives the model calculated concentrations. Next to this is a column containing the measured, normalized concentrations derived from the raw data. Finally, the far right column lists the squares of the errors given by the following formula:

$$E_i^2 = (C_{m,i}^* - C_i^*)^2 \quad (5.5)$$

where: E_i^2 = square of error at depth i

$C_{m,i}^*$ = model prediction of concentration at depth i

C_i^* = measured value of concentration at depth i

Core C			
Parameters from regression			
Biodiffusivity (D)	0.4561	cm ² /yr	
Depth adjustment	0.0801	cm	
Data regression			
Depth	Calculated	Actual	error
0.159	0.0775747	0.080860	1.0796E-05
0.318	0.0483858	0.043297	2.5893E-05
0.476	0.0220592	0.025243	1.0137E-05
0.634	0.0073508	0.002160	2.6942E-05
0.793	0.0017904	0.016338	0.00021162
0.951	0.0003187	0.024141	0.0005675
1.109	0.0000415	0.010622	0.00011196
1.268	0.0000039	0.004887	2.3843E-05
1.426	0.0000003	-0.003371	1.1363E-05
1.584	0.0000000	-0.000824	6.7966E-07
1.743	0.0000000	0.000000	0
1.901	0.0000000	0.000000	0
2.059	0.0000000	0.000000	0
yavg	0.0156	Error	0.0010
(y-yavg) ²	0.0059	R ²	0.8294

Figure 5.8 Example Spreadsheet Set Up for Data Regression

Regression is carried out on the data to minimize the sum of the squares of the errors by adjusting the values of the biodiffusion coefficient and the depth adjustment parameter.

With a good equation solver, this generally takes only a few seconds. In the case of an especially irregular profile, it may be necessary to add a constraint to prevent the value of D_b from becoming too small since it appears in the denominator of the solution term.

A statistical goodness of fit parameter similar to a correlation coefficient is defined and used to measure the improvement of the model fit over a straight line through the mean value of the normalized concentrations. This “pseudo-correlation coefficient” is defined by the following formula:

$$R^2 = \frac{\sum_i (C_i^* - \bar{C}^*)^2 - \sum_i E_i^2}{\sum_i (C_i^* - \bar{C}^*)^2} = 1 - \frac{\sum_i E_i^2}{\sum_i (C_i^* - \bar{C}^*)^2} \quad (5.6)$$

where: \bar{C}^* = average value of normalized concentration, cm^{-3}

A perfect fit is a curve that exactly matches the data and, therefore, has a sum of the squared errors of zero. This corresponds to an R^2 value of one. In the event that R^2 has a value of zero, the model has failed to improve the fit given by a straight line through the average value. In general, a good fit is taken to mean an R^2 value greater than 0.9, with values above 0.75 indicating a strong correlation.

5.5 Presentation of Results

5.5.1 Example Model Fits

Figures 5.9, 5.10, and 5.11 show the model fit of concentration-depth profiles for the three example cores with their tail sections removed. Figure 5.9 clearly depicts the influence of the data in the upper layers on overall curve shape. The regression analysis forces the curve through this point, in order to minimize the sum of the squares of the errors. Very little scatter is observed in the data and the first three layers are virtually on the model curve. In this regard it is also important to note the low amount of influence that points further into the sediments possess. Using points in the tail section as part of the regression would tend to slightly increase the values of D_b in order to maximize R^2 values. Figure 5.12 shows core 'C' from experiment 2 regressed with the entire tail section present. Note that the effect the tail section has on R^2 is small, and D_b has remained the same. In figure 5.11 we see the disadvantage to being unable to obtain both accurate initial profiles and time-progressed profiles from the same core. Since core 'C' in experiment 1 displays tracer profiles not typical of diffusive transport mechanisms, we are left to assume that either the

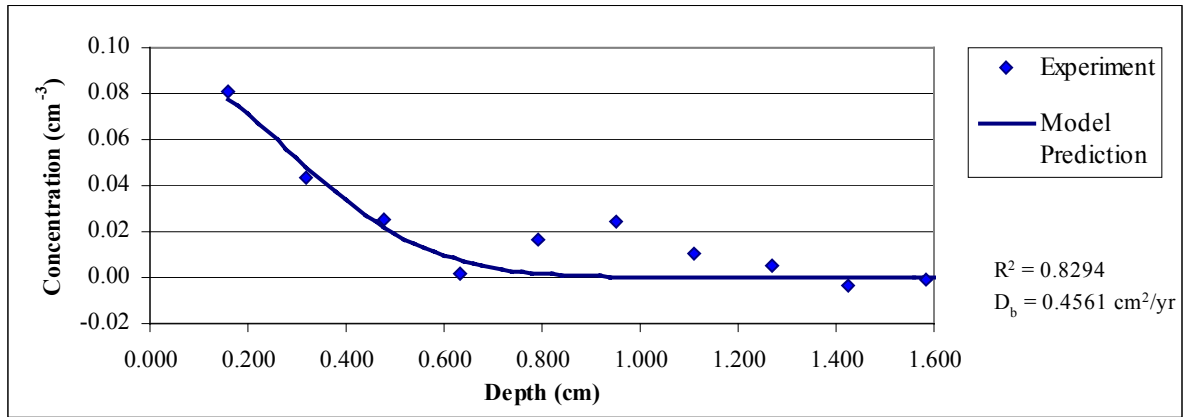


Figure 5.9 Model Fit of Concentration-Depth Profiles for Experiment 2, Core ‘C’

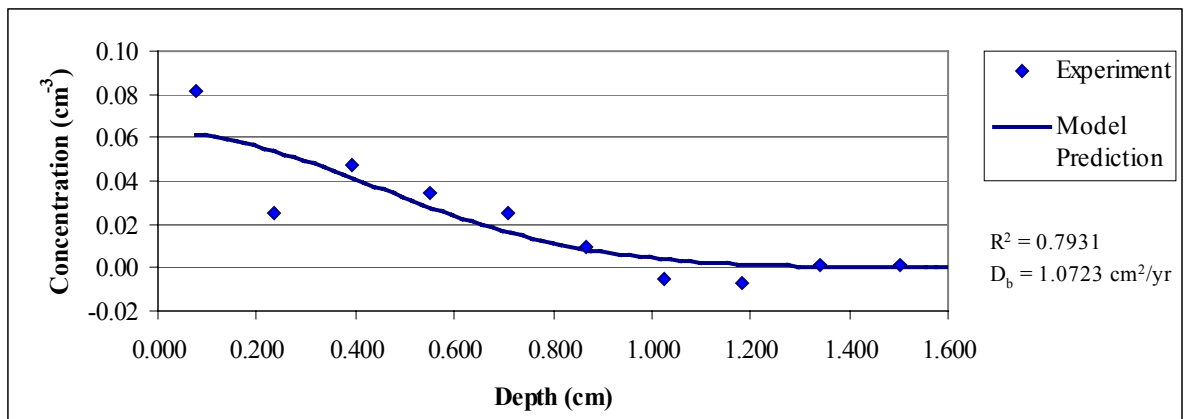


Figure 5.10 Model Fit of Concentration-Depth Profiles for Experiment 3, Core ‘B’

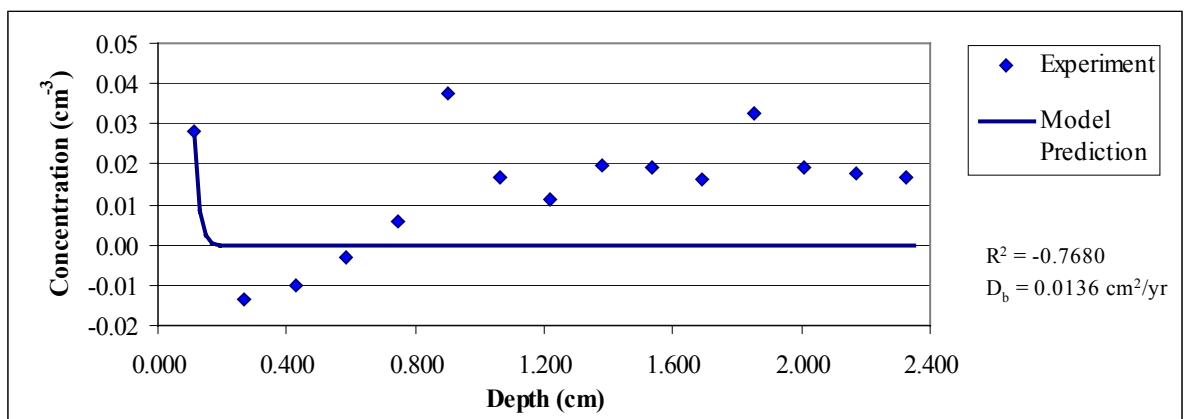


Figure 5.11 Model Fit of Concentration-Depth Profiles for Experiment 1, Core ‘C’

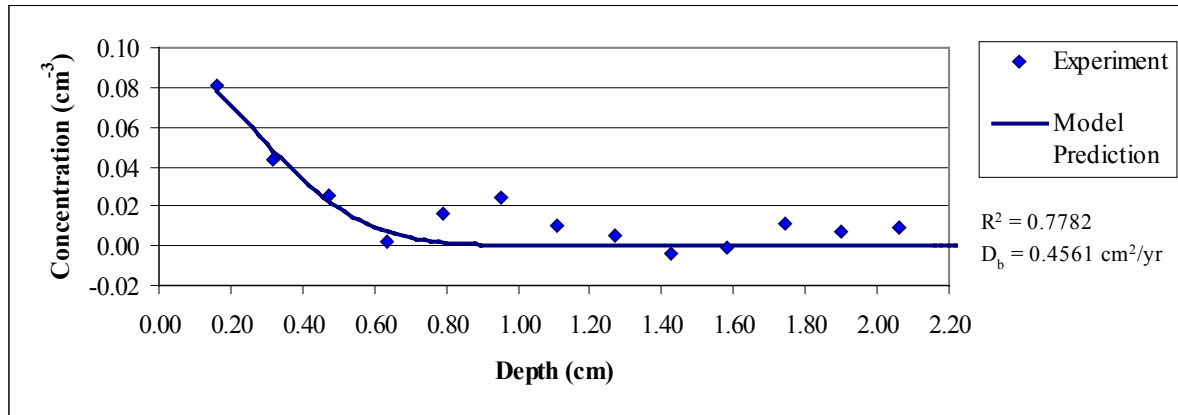


Figure 5.12 Model Fit With Tail Section for Experiment 2, Core ‘C’

initial profile was also atypical, other modes of bioturbation were occurring within the cored sediment, or that artifacts arising from sampling or handling techniques were introduced. Using the composite initial profile found in section 5.3, the second, third, and fourth data points are found to have “negative” concentrations, a physically unrealizable situation. This tends to fit the value of D_b towards a value of zero without accurately modeling the data. The calculated R^2 value is likewise negative, indicating an extremely poor fit. In this case, D_b is an order of magnitude lower than other values found during the same experiment. In interpreting the final results, the value of the biodiffusion coefficient measured from this core should be excluded from the mean.

5.5.2 Final Results of Tracer Experiments

Table 5.3 shows the results from model curve fits for five replicates analyzed from experiment 1, conducted during the month of December 2001. Likewise, Tables 5.4 and 5.5 show results from model curve fits for experiments 2 and 3, conducted during the months of January and February 2002. For each replicate, regressed parameters D_b and z_0 , the biodiffusion coefficient (in cm^2/yr) and the depth adjustment parameter (in cm), are shown. Along with these are values of the pseudo-correlation coefficient, R^2 , to present some degree

Table 5.3 Model Results and Statistics for Experiment 1, December 2001

	Biodiffusion Coeff (cm²/yr)	Depth Adjustment (cm)	R² for curve
Core 'A' [‡]	0.1245	0.0819	0.7600
Core 'B'	0.8900	-0.1406	0.7029
Core 'C' ^{‡‡}	0.0136	0.0317	-0.7680
Core 'D'	1.2305	0.0534	0.9393
Core 'E'	0.7281	-0.0591	0.8925
Mean	0.5973	-0.0065	-
Standard Deviation	0.5167	0.0917	-
Statistically Modified Mean	0.7433	0.0270	-
Statistically Modified Std. Dev.	0.4626	0.0610	-
Experimentally Modified Mean	0.9495	0.0270	-
Experimentally Modified Std. Dev.	0.2565	0.0610	-

Table 5.4 Model Results and Statistics for Experiment 2, January 2002

	Biodiffusion Coeff (cm²/yr)	Depth Adjustment (cm)	R² for curve
Core 'A' [‡]	0.5094	0.0130	0.4584
Core 'B' [‡]	0.1461	0.1031	0.5290
Core 'C'	0.4561	0.0801	0.8294
Core 'D' [†]	0.7883	0.0723	0.6656
Core 'E' [†]	0.1255	0.0662	0.8746
Mean	0.4051	0.0669	-
Standard Deviation	0.2764	0.0332	-
Statistically Modified Mean	0.3705	0.0654	-
Statistically Modified Std. Dev.	0.1962	0.0468	-
Experimentally Modified Mean	0.4566	0.0729	-
Experimentally Modified Std. Dev.	0.3314	0.0070	-

of goodness of fit for the parameters. Below this, statistical values for the mean biodiffusion coefficient and depth adjustment parameter, along with standard deviations of each, are shown. Then, the statistically adjusted means and standard deviations are shown. These values reflect the mean and standard deviation recalculated using just the values of D_b and z_0 that fall inside the range of the original mean plus or minus the original standard deviation. Finally, the experimentally adjusted mean and standard deviation are shown in which the

Table 5.5 Model Results and Statistics for Experiment 3, February 2002

	Biodiffusion Coeff (cm²/yr)	Depth Adjustment (cm)	R² for curve
Core 'A'^{†‡}	1.8588	-0.1492	0.6950
Core 'B'	1.0723	-0.0032	0.7931
Core 'C'	0.0833	-0.0050	0.9759
Core 'D'	0.3036	-0.0650	0.8590
Core 'E'^{†‡}	0.6015	-0.0772	0.8111
Mean	0.7839	-0.0599	-
Standard Deviation	0.7060	0.0603	-
Statistically Modified Mean	0.5152	-0.0376	-
Statistically Modified Std. Dev.	0.4279	0.0390	-
Experimentally Modified Mean	0.6591	-0.0484	-
Experimentally Modified Std. Dev.	0.3876	0.0397	-

values of suspect data were excluded from the calculation. Data that was excluded from the statistically adjusted mean and standard deviation are indicated by a † beside the core name. Similarly, data excluded from the experimentally adjusted mean and standard deviation are indicated by a ‡ beside the core name.

Biodiffusion coefficients calculated from Experiment 1 data have a mean value of 0.5973 ± 0.5167 cm²/yr, or 0.7433 ± 0.4626 cm²/yr after discarding core 'C' results for being outside of the one standard deviation range from the mean. However, the biodiffusion coefficient value for core 'A' seems to be nearly an order of magnitude lower than for other cores and thus has been eliminated from the experimentally modified mean. After removing this value from the data, the mean (experimentally modified mean) becomes 0.9495 ± 0.2565 cm²/yr. Average depth adjustment is -0.0065 ± 0.0917 cm, or 0.0270 ± 0.0610 cm after removing cores 'A' and 'C' from the calculation. This value, probably due to sedimentation and discrepancies in the top slice (may not have been quite as thick as lower slices due to limitations of the equipment), is quite reasonable, as sedimentation rates are estimated to be less than 3 cm/yr (0.25 cm/month) and are probably highly seasonal at this

point in the lake (DeLaune *et. al.*, 1989). Recent measures to reduce sedimentation may have additionally reduced this number. Inspection of pseudo-correlation coefficient values of the five curve fits indicates that all are reasonable except for core 'C'.

Experiment 2 returns a mean biodiffusion coefficient of $0.4051 \pm 0.2764 \text{ cm}^2/\text{yr}$, or $0.3705 \pm 0.1962 \text{ cm}^2/\text{yr}$ after discarding results from cores 'D' and 'E' as outliers. Despite the statistical soundness of cores 'A' and 'B', R^2 values for both indicate that a good fit was not achieved with the model and thus their results were excluded from the experimentally modified mean. This raises the overall value of the biodiffusion coefficient slightly to $0.4566 \pm 0.3314 \text{ cm}^2/\text{yr}$. Again, depth adjustment parameters seem reasonable but possibly a bit low at $0.0669 \pm 0.0332 \text{ cm}$, or $0.0654 \pm 0.0468 \text{ cm}$ after discarding cores 'D' and 'E'. The experimentally modified mean value of the depth adjustment parameter is slightly higher for experiment 2, $0.0729 \pm 0.0070 \text{ cm}$. The pseudo-correlation coefficients indicate good fits for cores 'C', 'D', and 'E' whereas cores 'A' and 'B' are not as good.

Experiment 3 showed a higher degree of inconsistency than the other two, giving a mean biodiffusion coefficient of $0.7839 \pm 0.7060 \text{ cm}^2/\text{yr}$, before discarding data points. However, after discarding core 'E' for being outside of the one standard deviation range and core 'A' for its relatively low value of the pseudo-correlation coefficient and high measured value of the biodiffusion coefficient, the mean value is found to be $0.6591 \pm 0.3876 \text{ cm}^2/\text{yr}$. It should be noted that the depth adjustment parameter, found to be $-0.0484 \pm 0.0397 \text{ cm}$ after modification, is again within reason given the researched value of 3 cm/yr observed by DeLaune *et. al.* (1989).

5.5.3 Discussion of Final Results

Even though biodiffusion coefficients are known to fluctuate seasonally, the consistency of the results for December, January, and February at the Capitol Lake Site indicate that the magnetite tracer technique was successful at quantifying the effects of bioturbation. However, it was difficult to obtain good estimations with a high degree of confidence due to the large number of significant environmental and experimental factors that influenced the final profiles used in the model. Also, because good data cores were difficult to retrieve for a number of reasons, it would be best to use more than five replicates for future work, perhaps even twice that number, in determining final biodiffusion coefficients. This was apparent in the fact that for each experiment, final parameter values of the experimentally modified mean were found using just three experimental data values. Nevertheless, based on the data and discussion a value of $0.68 \text{ cm}^2/\text{yr}$ with a range of $0.45 \text{ cm}^2/\text{yr}$ to $0.95 \text{ cm}^2/\text{yr}$ can be assigned to Capitol Lake

Table 5.6 Analysis of Variance for Experimental Results

Source of Variation	Degrees of Freedom	Sum of Squares	Mean Squares	F-Ratio
Mean	1	4.265	4.265	
Among Experiments	2	0.368	0.184	0.1696
Within Experiments	6	0.652	0.108	
Total	9	5.285		

In attempting to track any trends in the values of the three seasonal measurements, an analysis of variance was performed on the three experiments. Results of this analysis are shown in Table 5.6. The analysis of variance tested the hypothesis that the three distributions are statistically the same within a given amount of certainty, chosen arbitrarily to be 90%. This was accomplished by calculating an F-ratio from the given data and

comparing it to tabulated values in the literature. Values in the table for degrees of freedom were calculated according to the following formulas:

$$d_a = k - 1 \quad (5.7)$$

$$d_w = \sum_{i=1}^k (n_i - 1) \quad (5.8)$$

where: d_a = degrees of freedom among experiments

d_w = degrees of freedom within experiments

k = number of experiments being compared

n_i = number of observations in experiment i

Values for the sum of squares terms were found using the following formulas:

$$T = \sum_{i=1}^k \sum_{j=1}^{n_i} Y_{ij} \quad (5.9)$$

$$G_i = \sum_{j=1}^{n_i} Y_{ij} \quad (5.10)$$

$$M_{yy} = T^2 / \sum_{i=1}^k n_i \quad (5.11)$$

$$G_{yy} = \sum_{i=1}^k G_i^2 / n_i - M_{yy} \quad (5.12)$$

$$W_{yy} = \sum_{i=1}^k \sum_{j=1}^{n_i} Y_{ij}^2 - M_{yy} - G_{yy} \quad (5.13)$$

where: T = sum of data points from all experiments

Y_{ij} = individual data point j in experiment i

G_i = total of data points in experiment i

M_{yy} = Sum of squares of mean values for all experiments

G_{yy} = Sum of squares among experiments

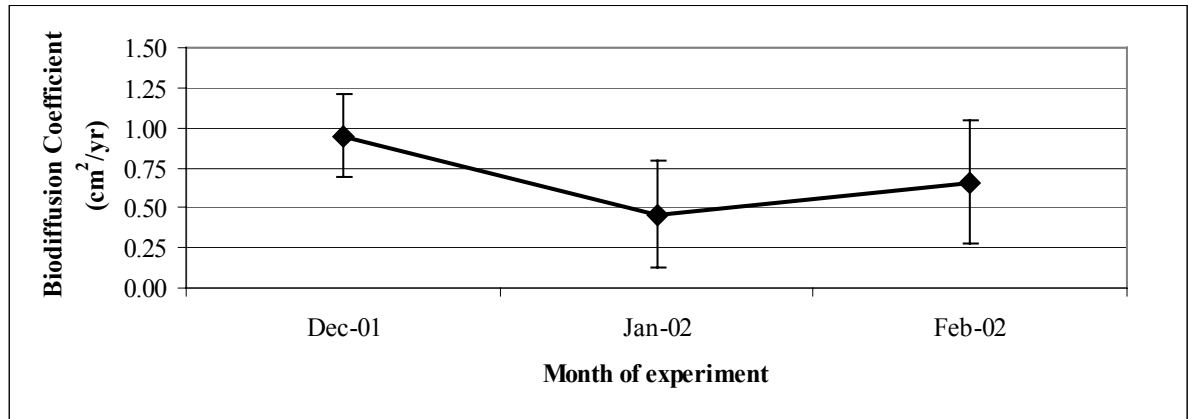


Figure 5.13 Calculated Values of Biodiffusion Coefficients vs. Month

$$W_{yy} = \text{Sum of squares within experiments}$$

From these values, Mean squares were found by dividing the appropriate sum of squares by the corresponding degrees of freedom (i.e. mean sum of squares by 1, sum of squares among groups by d_a , and sum of squares within groups by d_w .) The F-ratio was calculated according to the formula:

$$F = G/W \quad (5.14)$$

where: G = Mean square among groups

W = Mean square within groups

To be 90% certain that the three sets of experimental sample points with two degrees of freedom among groups and six degrees of freedom within groups were equal, the calculated F-ratio had to be less than 0.107 (Ostle, 1963). Since the calculated value of the F-ratio (1.696) was much greater than the required value, the hypothesis that the three means are equal was rejected. A graph showing the three experimental distributions appears in figure 5.13.

Several researchers in the literature have calculated biodiffusion coefficients for freshwater environments using various methods of data analysis. Guinasso and Schink

(1975) calculated values of D_b to be $1.38 \text{ cm}^2/\text{yr}$ for *Tubifex* oligochaetes in freshwater lakes. Robbins *et. al.* (1979) conducted experiments with tubificid oligochaetes similar to the ones found in Capitol Lake, but determined that their mixing capabilities were better described by an advective velocity parameter rather than by a biodiffusion coefficient. Fisher *et. al.* (1980) calculated D_b values from laboratory experiments with the worm *Tubifex tubifex* to be $2.74 \text{ cm}^2/\text{yr}$; however, Matisoff (1982) performed experiments with similar conditions and the same species of oligochaetes and found values of around $44.2 \text{ cm}^2/\text{yr}$, an order of magnitude higher. Officer and Lynch (1982) calculated values of D_b from the long half-live radiotracers ^{137}Cs and $^{239,240}\text{Pu}$ in the Great Lakes region, North America. Values ranged from as low as $0.05 \text{ cm}^2/\text{yr}$ for an area in the Belham Tarn to as high as $3 \text{ cm}^2/\text{yr}$ in the central basin of Lake Erie. Bukata and Bobba (1984) also conducted studies on the Great Lakes and found values of D_b to be in the range of $1.8 \text{ cm}^2/\text{yr}$ to $29.96 \text{ cm}^2/\text{yr}$. Keafer *et. al.* (1992) conducted experiments using ^{210}Pb profiles on Perch Pond in Falmouth, MA, and values of D_b were found to be $2.8 \text{ cm}^2/\text{yr}$. From these results it is apparent that values of biodiffusion coefficients are greatly a function of the region being sampled as well as the techniques and conditions of the experiments.

Much more extensive research has been conducted to calculate biodiffusion coefficients in marine environments. Martin and Sayles (1986) found cold-season average values of D_b to be $5.6 \text{ cm}^2/\text{yr}$ and warm-season averages to be $17 \text{ cm}^2/\text{yr}$ in nearshore sediments off the coast of Massachusetts. These values are an order of magnitude higher than those found by most freshwater research, almost certainly due to the larger and more diverse numbers of benthic organisms found in marine environments. Also, their model was much simpler due to the steady-state assumption used with naturally occurring, short-lived

radiotracers. They did, however, report a biodiffusion coefficient for experiments using amphipods in a laboratory cell with densities of 16 000 m⁻² of 4.4 cm²/yr. Wheatcroft (1992) reported biodiffusion coefficients in deep ocean sediments of 0.1–1 cm²/yr, dependent upon particle size. Although he used the same model as used in this research, no attempts were made to correct for initial tracer profiles despite the use of small glass beads, which undoubtedly underwent some degree of passive settling into tubes and burrows in the sediment. DeMaster *et. al.* (1985) performed short-term experiments on the continental slopes off the coast of Nova Scotia using the ²³⁴Th/²³⁸U disequilibrium and calculated D_b values ranging from 1.2 cm²/yr and 27 cm²/yr. Many additional values of D_b given in the literature have been summarized and converted to similar units by Thoms *et. al.* (1995).

The values of biodiffusion coefficients found by this research correlated well with the values published in the literature. According to Reible *et. al.* (1995), 2/3 of the published values of D_b given by Matisoff (1982) fell within the range of 0.3–30 cm²/yr. The fact that the values from this research fell within the lower part of that range was probably a direct result of the cold season in which the experiments were conducted and the relatively small bioturbating organisms (oligochaetes) found within Capitol Lake. Also, population densities of the worms in Capitol Lake were somewhat lower than those in other freshwater experiments. The overall effect is much slower mixing than in these other environments. Also, by failing to correct for passive deposition processes, many biodiffusion coefficients published in the literature may have incorporated both passive deposition and active mixing processes in the reported values of biodiffusion coefficients, giving them slightly inflated values. This becomes especially true for short-term tracer studies, which cannot “dampen” the effects of passive deposition during such short periods of time. Also, many studies were

performed with naturally occurring radiotracers assumed to have steady-state profiles in the sediment. Although calculation of these coefficients is more straightforward, the results are entirely dependent on the steady-state assumption of the model being true.

Chapter 6

Conclusions and Recommendations

6.1 Conclusions

Experiments conducted in the sediments of South Capitol Lake indicate that magnetite can be used successfully to measure biodiffusion coefficients. The benefits of using the newly developed magnetite tracer protocol include the low cost of materials, the short timescales involved in conducting successful experiments, and the lack of requirements for expensive or specialized analytical equipment; however, data was difficult to obtain, and often varied greatly within the same sample plot. Also, because tracer coverage resulting from the existing broadcasting technique was not uniform at the sediment surface, some improvements are needed to increase the accuracy of results. Results obtained for the three experiments conducted as part of this research and biodiffusion coefficients values calculated were consistent with values reported in the literature for freshwater environments. Furthermore, the fact that consistent initial tracer depth distributions existed as the result of passive deposition into pore structures was discovered. The method presented for correcting final data to account for such distributions resulted, in most cases, in reasonable final concentration-depth profiles. This technique was also capable of dampening the effects of background concentrations and sampling artifacts, since the sampling techniques used initially and at 30 days were identical. Finally, the unsteady-state diffusion model proved acceptable in most cases to give a good visual and statistical fit to final concentration-depth profiles calculated from experimental data.

Some difficulties were encountered during the research. In areas where submerged aquatic vegetation was fairly dense, magnetite was unable to penetrate through it to reach

the sediment-water interface. Tracer loadings found in retrieved cores were less than those that would have resulted from uniform tracer coverage by the amount of magnetite deployed over each data plot. Furthermore, the broadcasting technique did not work well in areas where plant debris was concentrated in the sediment, or where the top sediment layer was uneven. Further, because the final tracer distributions depend upon so many environmental factors, often several of the data core replicates were discarded due to poor or irregular concentration-depth profiles and the final values of biodiffusion coefficients were based upon a small number of data profiles.

6.2 Recommendations

Some future research should be dedicated to applying the magnetite tracer technique to study the seasonal variations of biodiffusion coefficients in lakes. Unlike other tracer techniques, which operate on timescales of many months to years, the magnetite tracer technique is capable of working over timescales short enough to detect monthly fluctuations in biodiffusion coefficients. Ideally, some correlation for biodiffusion coefficients as a function of time of the year could be developed for particular water bodies or sections thereof. This is especially useful for improving the seasonal accuracy of chemical fate and transport models, which require these coefficients in order to assess the natural recovery potential for contaminated sediment zones.

Future research should include tracer studies for time periods longer than 30 days to test any time limitations of the technique that might exist and observe the effectiveness of the tracer technique for extended time periods. Another important task is the development of a method for overcoming difficulties encountered when conducting experiments in the presence of submerged aquatic vegetation. Some time should be invested into improving

the tracer broadcasting technique, since low tracer loadings and difficulties spreading tracers over plots account for many problems with final data analyses. Developing a method of preparing data plots *in situ* via underwater scuba divers would probably eliminate many of the problems arising from non-uniform coverage by magnetite and interference from submerged aquatic vegetation. This would also improve the ability of researchers to obtain data cores with even surface topographies, and would eliminate samples that miss the data plot. Once a method employing scuba divers was developed, magnetite with a smaller average particle diameter should be used to more closely simulate the natural sediment, which typically has an average particle diameter less than 50 μm .

Analytical procedures for measuring concentration-depth profiles in retrieved data cores need to be improved as well. Design and construction of a device capable of precision extrusion of the mud core in increments much less than the 1.5 mm increments used in this research would greatly improve the accuracy with which biodiffusion coefficients could be calculated. This would also eliminate problems associated with the inexact alignment of the core surface with the top of the coring tube caused by limitations of the spacers used in slicing the cores.

References

- Aller, Robert C., and Kirk Cochran. 1976. “ $^{234}\text{Th}/^{238}\text{U}$ Disequilibrium in Near-Shore Sediment: Particle Reworking and Diagenetic Time Scales.” *Earth Planet. Sci. Lett.*, 29, 37–50.
- Aller, Robert C., Larry K. Benninger, and Kirk Cochran. 1986. “Tracking Particle-Associated Processes in Near-Shore Environments by Use of $^{234}\text{Th}/^{238}\text{U}$ Disequilibrium.” *Earth Planet. Sci. Lett.*, 47, 161–175.
- Aller, Robert C. 2001. “Transport and Reactions in the Bioirrigated Zone.” Chapter 11 in Bernard P. Boudreau and Bo Barker Jørgensen, eds. *The Benthic Boundary Layer*. Oxford University Press: New York, 269–301.
- Benninger, L. K., R. C. Aller, J. K. Cochran, and K. K. Turekian. 1979. “Effects of Biological Sediment Mixing on the ^{210}Pb Chronology and Trace Metal Distribution in a Long Island Sound Sediment Core.” *Earth Planet. Sci. Lett.*, 43, 241–259.
- Berner, Robert A. 1980. *Early Diagenesis*. Princeton University Press: Princeton, NJ, 224 pp.
- Blasland, Bouck & Lee, Inc. 2000. “Analysis of Sources and Fate of PCBs in the Grasse River and Assessment of Natural Recovery and the Effectiveness of Remediation.” pp. 3-51.
- Bukata, R. P. and A. G. Bobba. 1984. “Determination of Diffusion Coefficients Associated with the Transport of ^{210}Pb Radionuclides in Lake Bed Sediments.” *Environ. Geol.*, 5, 133.
- Carey, Drew A. 1989. “Fluorometric Detection of Tracer Particles Used to Study Animal-Particle Dynamics.” *Limnol. Oceanogr.*, 34, 630–635.
- Choy, Bruce and Danny D. Reible. 2000. “Diffusion Models of Environmental Transport.” Lewis Publishers: Boca Raton, FL, 183 pp.
- Connolly, J. P., et. al.. 2000. “A Model of PCB Fate in the Upper Hudson River. *Env. Sci. Tech.*, 34, 4076.
- Crank, J. 1975. “The Mathematics of Diffusion.” Clarendon Press: Oxford, 414 pp.
- DeLaune, R. D., R. P. Gambrell, and R. S. Knox. 1989. “Accumulation of Heavy Metals and PCB’s in an Urban Lake.” *Env. Tech. Lett.*, 10, 753–762.
- DeMaster, D. J., B. A. McKee, C. A. Nittrouer, D. C. Brewster, and P. E. Biscaye. 1985. “Rates of Sediment Reworking at the HEBBLE Site Based on Measurements of ^{234}Th , ^{137}Cs , and ^{210}Pb .” *Mar. Geology*, 66, 133.

- Fisher, J. B., W. J. Lick, P. L. McCall, and J. A. Robbins. 1980. "Vertical Mixing of Lake Sediments by Tubificid Oligochaetes." *J. Geophys. Res.*, 83, 3997.
- Fitzgerald, Sharon A., J. Val Klump, Peter W. Swarzenski, Richard A. Mackenzie, and Kevin D. Richards. 2001. "Beryllium-7 as a Tracer of Short-Term Sediment Deposition and Resuspension in the Fox River, Wisconsin." *Env. Sci. Tech.*, 35, pp. 300–305.
- Fornes, W. L., D. J. DeMaster, L. A. Levin, and N. E. Blair. 1999. "Bioturbation and Particle Transport in Carolina Slope Sediments: A Radiochemical Approach." *J. Mar. Res.*, 57, 335–355.
- Gerino, Magali. 1990. "The Effects of Bioturbation on Particle Redistribution in Mediterranean Coastal Sediment. Preliminary Results." *Hydrobiologia*, 207, 251–258.
- Gerino, Magali, Georges Stora, and Jean-Pierre Durbec. 1994. "Quantitative Estimation of Biodiffusive and Bioadvective Sediment Mixing: *In Situ* Experimental Approach." *Oceanologica Acta*, 17, 547–554.
- Goldberg, E. D., and M. Koide. 1962. "Geochronological Studies of Deep-Sea Sediments by the Ionium/Thorium Method." *Geochim. Cosmochim. Acta*, 26, 417–450.
- Guinasso, N. L., and Schink, D. R. 1975. "Quantitative Estimates of Biological Mixing Rates in Abyssal Sediments." *J. Geophys. Res.*, 80, 3032.
- Henderson, Gideon M., Fara N. Lindsay, and Niall C. Slowey. 1999. "Variation in Bioturbation with Water Depth on Marine Slopes: A Study on the Little Bahamas Bank." *Mar. Geol.*, 160, 105–118.
- Kershaw, P. J., D. J. Swift, R. J. Pentreath, and M. B. Lovett. 1984. "The Incorporation of Plutonium, Americium, and Curium Into the Irish Sea Seabed by Biological Activity." *Sci. Total Environ.*, 40, 61–81.
- Lee, Henry II, and Richard C. Swartz. 1980. "Biological Processes Affecting the Distribution of Pollutants in Marine Sediments. Part II. Biodeposition and Bioturbation." Chapter 29 in R. A. Baker, ed., *Contaminants and Sediments, vol. 2 Analysis, Chemistry, Biology*. Ann Arbor Science: Ann Arbor, MI, 555–594.
- Limno-Tech, Inc. 1999. "Addendum to Development of Alternative Suite of Models for the Lower Fox River." Ann Arbor, MI, p. 30.
- Lotufo, G. R., and J. W. Fleeger. 1996. "Toxicity of sediment-associated pyrene and phenanthrene to *Limnodrilus hoffmeisteri* (Oligochaeta: Tubificidae)." *Environ. Toxicol. Chem.*, 15, 1508–1516.
- Mahaut, Marie-Laure, and Gerhard Graf. 1987. "A Luminophore Tracer Technique for Bioturbation Studies." *Oceanologica Acta*, 10, 323–328.

- Martin, W. R., and F. L. Sayles. 1987. "Seasonal Cycles of Particle and Solute Transport Processes in Nearshore Sediments: $^{222}\text{Rn}/^{226}\text{Ra}$ and $^{234}\text{Th}/^{238}\text{U}$ Disequilibrium at a Site in Buzzards Bay, MA." *Geochim. Cosmochim. Acta*, 51, 927–943.
- Matisoff, Gerald. 1982. "Mathematical Models of Bioturbation." In *Animal-Sediment Relations, The Biogenic Alteration of Sediments*. P. L. McCall and M. J. S. Tevesz, eds. Plenum Press: New York.
- Mazik, Krystina, and M. Elliott. 2000. "The Effects of Chemical Pollution on the Bioturbation Potential of Estuarine Intertidal Mudflats." *Helgol Mar. Res.*, 54, 99–109.
- Meadows, P. S., and J. G. Anderson. 1966. "Micro-Organisms Attached to Marine and Freshwater Sand Grains." *Nature*, 212, 1059–1060.
- Mohanty, Sanat. 1997. "Modeling of Fate and Transport of Contaminants Under the Influence of Bioturbation." Master of Science in Chemical Engineering Thesis, Louisiana State University, 96 pp.
- Myers, Keith R., and Kevin J. Poché. 1988. *Potential Sources of Various Pollutants Found in Capitol Lake Sediment*. Public Document, Louisiana Department of Environmental Quality Inactive and Abandoned Sites Division, 21 pp.
- National Research Council. 2001. "A Risk Management Strategy for PCB Contaminated Sediments."
- Officer, C. B. and D. R. Lynch. 1982. "Interpretation Procedures for the Determination of Sediment Parameters from Time-Dependent Flux Inputs." *Earth Planet. Sci. Lett.*, 61, 55.
- Olmez, Ilhan, Francis X. Pink, and Robert A. Wheatcroft. 1994. "New Particle-Labeling Technique for Use in Biological and Physical Sediment Transport Studies." *Environ. Sci. Technol.*, 28, 1487–1490.
- Ostle, Bernard. 1963. "Statistics in Research." The Iowa State University Press: Ames, IA. 585 pp.
- Reible, D. D., V. Popov, K. T. Valsaraj, L. J. Thibodeaux, F. Lin, M. Dikshit, M. A. Todaro, and J. W. Fleeger. 1995. "Contaminant Fluxes From Sediment Due To Tubificid Oligochaete Bioturbation." *Wat. Res.*, 30, 704–714.
- Rice, Donald L. 1986. "Early Diagenesis in Bioadvective Sediments: Relationships Between the Diagenesis of Beryllium-7, Sediment Reworking Rates, and the Abundance of Conveyor-belt Deposit-Feeders." *J. Mar. Res.*, 44, 149–184.
- Robbins, John A., Peter L. McCall, J. Berton Fisher, and John R. Krezoski. 1979. "Effect of Deposit Feeders on Migration of ^{137}Cs in Lake Sediments." *Earth Planet. Sci. Lett.*, 42, 277–287.

- Santschi, Peter H., Robert F. Anderson, and Martin Q. Fleisher. 1991. "Measurements of Diffusive Sublayer Thickness in the Ocean by Alabaster Dissolution, and Their Implications for the Measurements of Benthic Fluxes." *J. Geophys. Res.*, 96, 10641–10657.
- Smith, C. R., R. H. Pope, D. J. DeMaster, and L. Magaard. 1993. "Age Dependent Mixing of Deep Sea Sediments." *Geochim. Cosmochim. Acta*, 57, 1473–1488.
- Smith, Douglas G. 2001. "Annelida." Chapter 13 in *Pennak's Freshwater Invertebrates of the United States*, 4 ed. John Wiley & Sons, Inc.: New York. 269–325.
- Smith, J. N., and C. T. Schafer. 1984. "Bioturbation Processes in Continental Slope and Rise Sediments Delineated by Pb-210, Microfossil and Textural Indicators." *J. Mar. Res.*, 42, 1117–1145.
- Swift, D. J. 1993. "The Macrobenthic Infauna Off Selafield (North-Eastern Irish Sea) With Special Reference to Bioturbation." *J. Mar. Biol. Ass. U. K.*, 73, 143–162.
- TAMS Consultants, Inc., *et. al.* 2000. "Hudson River PCBs Reassessment RI/FS, Vol 2D- Revised Baseline Modeling Report, Phase 2 Review Copy." p. 147.
- Tedesco, L. P., and R. C. Aller. 1997. "²¹⁰Pb Chronology of Sequences Affected by Burrow Excavation and Infilling: Examples From Shallow Marine Carbonate Sediment Sequences, Holocene South Florida and Caicos Platform, British West Indies." *J. Sediment. Res. (A: Sediment. Petrol. Process.)*, 67, 36–46.
- Thibodeaux, Louis J., Kalliat T. Valsaraj, and Danny D. Reible. 2001. "Bioturbation-Driven Transport of Hydrophobic Organic Contaminants from Bed Sediment." *Env. Eng. Sci.*, 18, 215–223.
- Thibodeaux, Louis J. 2002. "Non-Particle Resuspension Chemical Transport from Stream Beds." in Robert L. Lipnick, Robert P. Mason, Margaret L. Phillips, and Charles U. Pittman, eds., *A.C.S. Symposium Series No. 806, Chemicals in the Environment: Fate, Impacts, and Remediation*. In press.
- Thoms, Sharon, Gerald Matisoff, Peter L. McCall, Xiaosong Wang, Andrew Stoddard, Martha Martin, V. Juanita Banks. 1995. "Models for Alteration of Sediments by Benthic Organisms." Water Environment Research Foundation Project 92-NPS-2.
- Wheatcroft, Robert A. 1992. "Experimental Tests for Particle Size-Dependent Bioturbation in the Deep Ocean." *Limnol. Oceanogr.*, 37, 90–104.
- Wheatcroft, Robert A., Ilhan Olmez, and Francis X. Pink. 1994. "Particle Bioturbation in Massachusetts Bay Preliminary Results Using a New Deliberate Tracer Technique." *J. Mar. Res.*, 52, 1129–1150.

Appendix

A.1 Overview

The purpose of the appendix is to present the complete results and analyses of individual experiments conducted during the course of this research. First, the results of the fecal matter collection experiment are presented. The next section shows the data for initial profiles used in data analysis. The final section contains results for the three benthic tracer studies, broken into three sections, one for each of the three experiments. For the sake of continuity, results from each experiment are grouped together from raw data to final concentration-depth profiles.

A.2 Fecal Matter Collection Experiments

Table A.1 shows the raw data collected from the analysis of bulk sediment used in the oligochaete selectivity experiments. Values of the mean sediment tracer concentration and its standard deviation are given in the last row below the sample concentrations. Table A.2 shows the individual sample analyses collected from the experiment.

Table A.1 Raw Data for Determination of Concentration in Bulk Sediment

Standard Concentration Determination					
Sample #	Sample Weight (g)	Dish Weight (g)	Sediment Weight (g)	Magnetite Weight (g)	Concentration (g mag/g sed)
1	2.1507	1.0639	1.0868	0.0447	0.0411
2	4.1140	1.0809	3.0331	0.1293	0.0426
3	3.9417	1.0706	2.8711	0.1054	0.0367
4	5.1505	1.0664	4.0841	0.1630	0.0399
5	5.6907	1.0818	4.6089	0.1863	0.0404
6	5.7315	1.0719	4.6596	0.1876	0.0403
Mean	-	-	-	-	0.0402 ± .0020

Table A.2 Sample Concentration Analysis and Comparison to Bulk Sediment

Standard Concentration Determination						
Sample #	Sample Weight (g)	Dish Weight (g)	Sediment Weight (g)	Magnetite Weight (g)	Concentration (g mag/g sed)	Ratio to bulk
1	1.3650	1.0782	0.2868	0.0050	0.0174	0.4337
2	1.1782	1.0790	0.0992	0.0026	0.0262	0.6520
3	1.5418	1.0835	0.4583	0.0081	0.0177	0.4397
4	1.3752	1.0879	0.2873	0.0096	0.0334	0.8312
Mean	-	-	-	-	0.0237 ± .0077	0.5891

A.3 Initial Profile Experiments

Table A.3 shows the raw weight-depth data from initial cores taken in Capitol Lake.

Table A.4 shows the results of data analysis performed on raw data from Table A.3

according to the procedure described in chapter 5. These values were used to obtain the initial profile used in adjusting data, shown in the far right column labeled “Average Conc.”

Figure A.1 is included here for convenience as a graphical picture of the initial core profiles.

Table A.3 Raw Data used to analyze initial tracer profiles

Raw Data from Initial Data Profiles					
Slice #	Depth Range (mm)	Average Depth (mm)	Core ‘A’ weight magnetite (g)	Core ‘B’ weight magnetite (g)	Core ‘C’ weight magnetite (g)
1	0.000-1.583	0.7917	0.076	0.111	0.126
2	1.583-3.167	2.3750	0.014	0.026	0.008
3	3.167-4.750	3.9583	0.008	0.039	0.022
4	4.750-6.333	5.5417	0.005	0.015	0.016
5	6.333-7.917	7.1250	0.006	0.009	0.016
6	7.917-9.500	8.7083	0.007	0.006	0.013
7	9.500-11.083	10.2917	0.006	0.004	0.012
8	11.083-12.667	11.8750	0.006	0.003	0.014
9	12.667-14.250	13.4583	0.007	0.004	0.008
10	14.250-15.833	15.0417	0.004	0.002	0.007
Loading	-	-	0.139	0.219	0.242

Table A.4 Initial Tracer Profile data

Normalized Initial Tracer Profiles						
Slice #	Depth Range (mm)	Average Depth (mm)	Core 'A' Conc. (cm ⁻³)	Core 'B' Conc. (cm ⁻³)	Core 'C' Conc. (cm ⁻³)	Average Conc. (cm ⁻³)
1	0.000-1.583	0.7917	0.5455	0.6128	0.5207	0.5736
2	1.583-3.167	2.3750	0.0959	0.1187	0.0331	0.0826
3	3.167-4.750	3.9583	0.0537	0.0722	0.0909	0.0772
4	4.750-6.333	5.5417	0.0491	0.0685	0.0661	0.0612
5	6.333-7.917	7.1250	0.0411	0.0411	0.0661	0.0494
6	7.917-9.500	8.7083	0.0479	0.0274	0.0537	0.0430
7	9.500-11.083	10.2917	0.0411	0.0183	0.0496	0.0363
8	11.083-12.667	11.8750	0.0411	0.0137	0.0579	0.0280
9	12.667-14.250	13.4583	0.0572	0.0183	0.0331	0.0268
10	14.250-15.833	15.0417	0.0274	0.0091	0.0289	0.0218

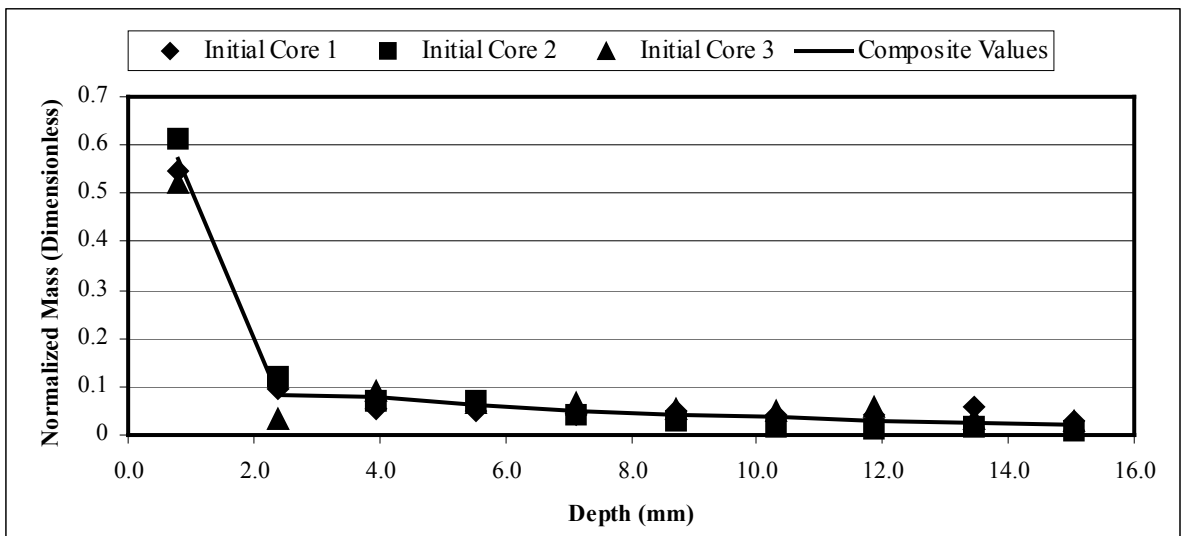


Figure A.1 Initial Concentration Profiles Used in Data Analysis.

A.4 Benthic Tracer Study Data

This section contains three sections, one for each of the experiments reported by this research. Each subsection contains the raw and adjusted raw data (see section 5.4) for a particular experiment, followed by the final regression model fitted to the data.

A.4.1 Experiment 1, Capitol Lake, December 2001

Table A.5 Raw Data for Experiment 1

Location			Weight of Magnetite (g)				
Slice #	Depth Range (mm)	Average Depth (mm)	Core 'A'	Core 'B'	Core 'C'	Core 'D'	Core 'E'
1	0.000-1.583	0.792	0.108	0.079	0.081	0.151	0.193
2	1.583-3.167	2.375	0.047	0.222	0.049	0.179	0.200
3	3.167-4.750	3.958	0.036	0.560	0.051	0.166	0.231
4	4.750-6.333	5.542	0.024	0.469	0.056	0.103	0.105
5	6.333-7.917	7.125	0.018	0.257	0.070	0.076	0.045
6	7.917-9.500	8.708	0.025	0.074	0.154	0.048	0.022
7	9.500-11.083	10.292	0.031	0.018	0.087	0.044	0.014
8	11.083-12.667	11.875	0.021	0.013	0.062	0.027	0.007
9	12.667-14.250	13.458	0.019	0.010	0.057	0.026	0.006
10	14.250-15.833	15.042	0.034	0.014	0.055	0.014	0.004
11	15.833-17.417	16.625	0.021	0.007	0.046	0.009	0.004
12	17.417-19.000	18.208	0.003	0.005	0.093	0.009	0.003
13	19.000-20.583	19.792	0.001	0.007	0.055	0.011	0.003
14	20.583-22.167	21.375	0.006	0.005	0.051	0.006	0.003
15	22.167-23.750	22.958	0.003	0.006	0.048	0.005	0.001
Total	-	-	0.388	1.723	1.015	0.843	0.823
Loading (g/cm³)	-	-	0.0218	0.0967	0.0570	0.0473	0.0462

Table A.6 Normalized Adjusted Concentrations for Experiment 1

Location			Normalized Adjusted Concentrations (cm ⁻³)				
Slice #	Depth Range (mm)	Average Depth (mm)	Core 'A'	Core 'B'	Core 'C'	Core 'D'	Core 'E'
1	0.000-1.583	0.792	0.0987	0.0163	0.0283	0.0635	0.0831
2	1.583-3.167	2.375	0.0121	0.0311	-0.0137	0.0444	0.0553
3	3.167-4.750	3.958	0.0049	0.0872	-0.0102	0.0418	0.0715
4	4.750-6.333	5.542	-0.0009	0.0736	-0.0033	0.0204	0.0224
5	6.333-7.917	7.125	-0.0020	0.0344	0.0060	0.0135	0.0009
6	7.917-9.500	8.708	0.0068	-0.0008	0.0377	0.0041	-0.0066
7	9.500-11.083	10.292	0.0148	-0.0099	0.0168	0.0049	-0.0075
8	11.083-12.667	11.875	0.0087	-0.0078	0.0112	0.0009	-0.0075
9	12.667-14.250	13.458	0.0174	0.0021	0.0199	0.0109	0.0026
10	14.250-15.833	15.042	0.0311	0.0029	0.0192	0.0059	0.0017
11	15.833-17.417	16.625	0.0192	0.0014	0.0161	0.0038	0.0017
12	17.417-19.000	18.208	0.0027	0.0010	0.0325	0.0038	0.0013
13	19.000-20.583	19.792	0.0009	0.0014	0.0192	0.0046	0.0013
14	20.583-22.167	21.375	0.0055	0.0010	0.0178	0.0025	0.0013
15	22.167-23.750	22.958	0.0027	0.0012	0.0168	0.0021	0.0004

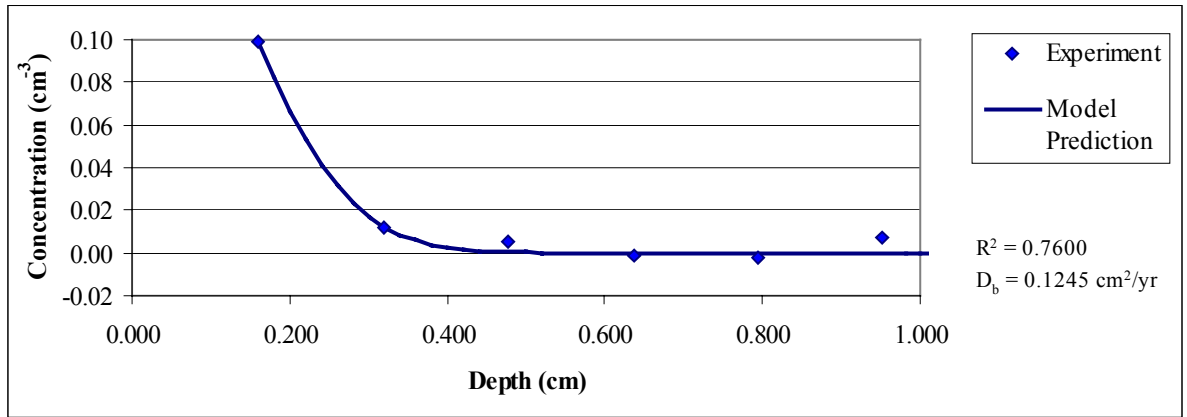


Figure A.2 Model Curve Fit to Core 'A', Experiment 1

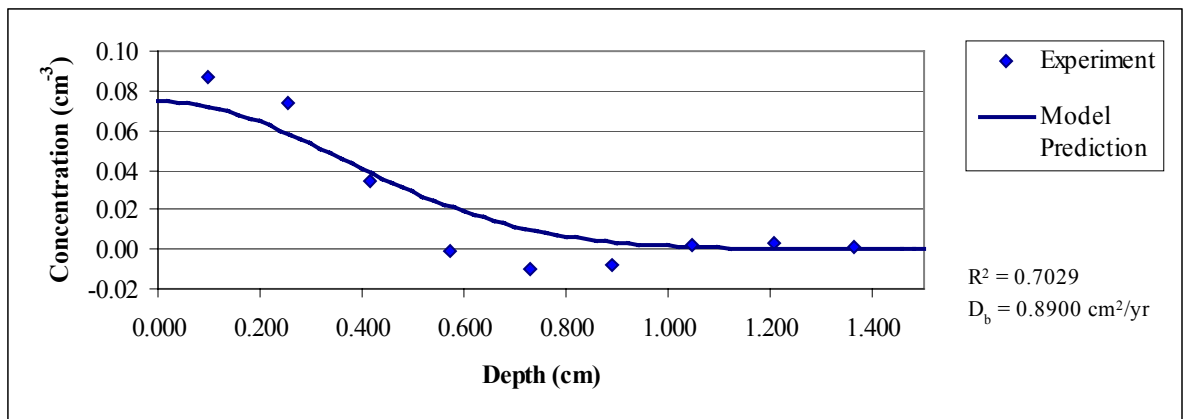


Figure A.3 Model Curve Fit to Core 'B', Experiment 1

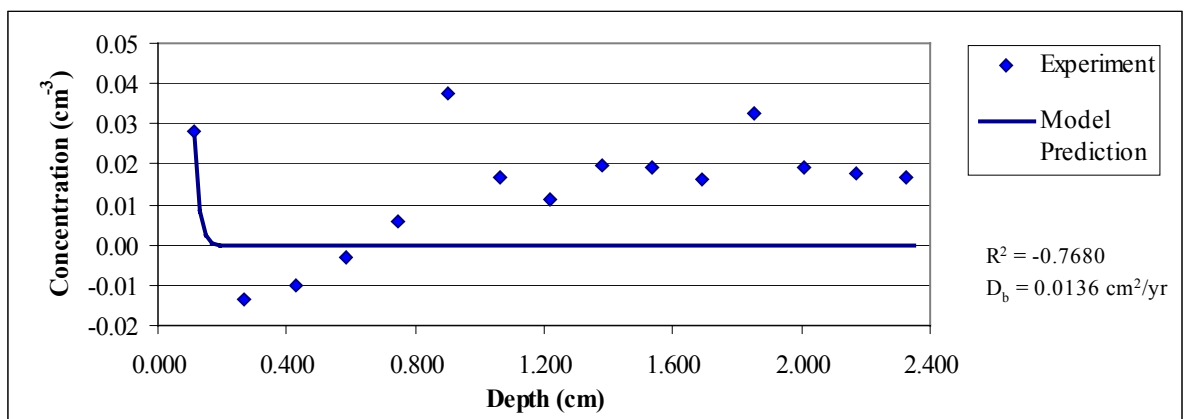


Figure A.4 Model Curve Fit to Core 'C', Experiment 1

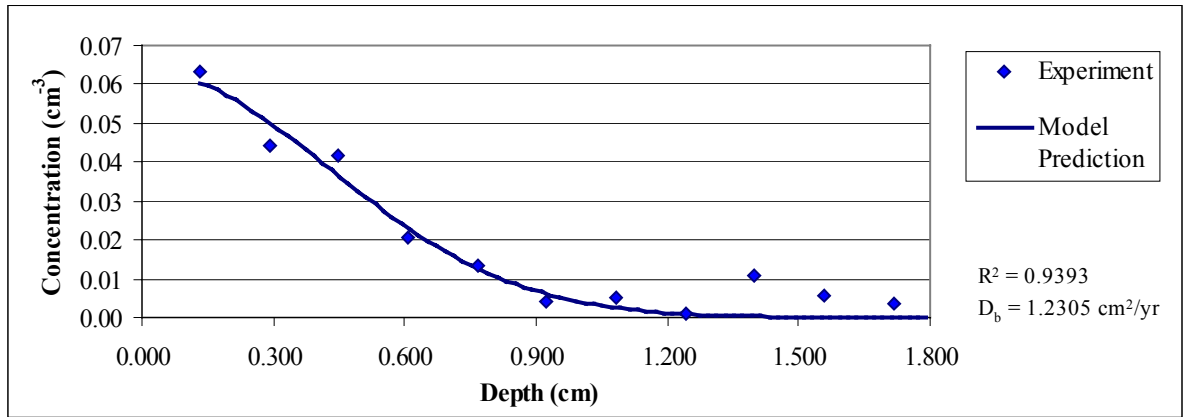


Figure A.5 Model Curve Fit to Core 'D', Experiment 1

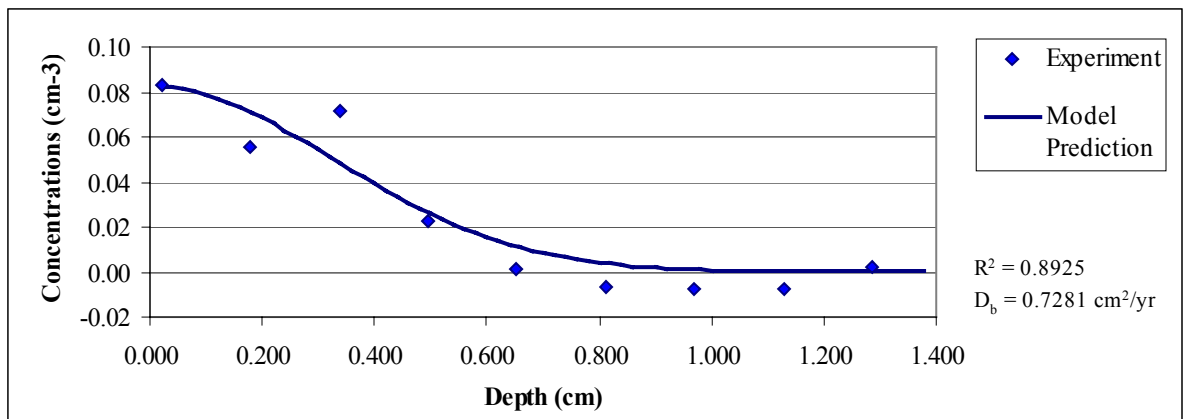


Figure A.6 Model Curve Fit to Core 'E', Experiment 1

A.4.2 Experiment 2, Capitol Lake, January 2002

Table A.7 Raw Data for Experiment 2

Location			Weight of Magnetite (g)				
Slice #	Depth Range (mm)	Average Depth (mm)	Core 'A'	Core 'B'	Core 'C'	Core 'D'	Core 'E'
1	0.000-1.583	0.792	0.039	0.037	0.117	0.061	0.216
2	1.583-3.167	2.375	0.119	0.020	0.105	0.040	0.096
3	3.167-4.750	3.958	0.314	0.013	0.075	0.064	0.088
4	4.750-6.333	5.542	0.028	0.016	0.032	0.020	0.031
5	6.333-7.917	7.125	0.018	0.018	0.049	0.021	0.067
6	7.917-9.500	8.708	0.068	0.024	0.057	0.020	0.040
7	9.500-11.083	10.292	0.086	0.016	0.034	0.022	0.051
8	11.083-12.667	11.875	0.016	0.006	0.024	0.007	0.033
9	12.667-14.250	13.458	0.033	0.006	0.010	0.016	0.038
10	14.250-15.833	15.042	0.023	0.008	0.010	0.007	0.051
11	15.833-17.417	16.625	0.014	0.005	0.016	0.006	0.069
12	17.417-19.000	18.208	0.014	0.004	0.010	0.005	0.112
13	19.000-20.583	19.792	0.008	0.004	0.013	0.012	0.024
14	20.583-22.167	21.375	0.008	0.005	0.014	0.016	0.032
15	22.167-23.750	22.958	0.006	0.007	0.024	0.004	0.024
Total	-	-	0.780	0.169	0.503	0.278	0.660
Loading (g/cm³)	-	-	0.0438	0.0095	0.0282	0.0156	0.0370

Table A.8 Normalized Adjusted Concentrations for Experiment 2

Location			Normalized Adjusted Concentrations (cm ⁻³)				
Slice #	Depth Range (mm)	Average Depth (mm)	Core 'A'	Core 'B'	Core 'C'	Core 'D'	Core 'E'
1	0.000-1.583	0.792	0.0186	0.0841	0.0809	0.0778	0.1077
2	1.583-3.167	2.375	0.0460	0.0162	0.0433	0.0217	0.0186
3	3.167-4.750	3.958	0.1231	0.0030	0.0252	0.0550	0.0173
4	4.750-6.333	5.542	-0.0064	0.0164	0.0022	0.0056	-0.0045
5	6.333-7.917	7.125	-0.0092	0.0234	0.0163	0.0093	0.0159
6	7.917-9.500	8.708	0.0172	0.0393	0.0241	0.0103	0.0047
7	9.500-11.083	10.292	0.0281	0.0235	0.0106	0.0152	0.0126
8	11.083-12.667	11.875	-0.0041	0.0019	0.0049	-0.0028	0.0048
9	12.667-14.250	13.458	0.0054	0.0034	-0.0034	0.0101	0.0087
10	14.250-15.833	15.042	0.0032	0.0104	-0.0008	0.0012	0.0177
11	15.833-17.417	16.625	0.0067	0.0114	0.0111	0.0077	0.0344
12	17.417-19.000	18.208	0.0067	0.0091	0.0069	0.0064	0.0558
13	19.000-20.583	19.792	0.0038	0.0091	0.0090	0.0153	0.0120
14	20.583-22.167	21.375	0.0038	0.0114	0.0097	0.0077	0.0160
15	22.167-23.750	22.958	0.0029	0.0159	0.0166	0.0051	0.0120

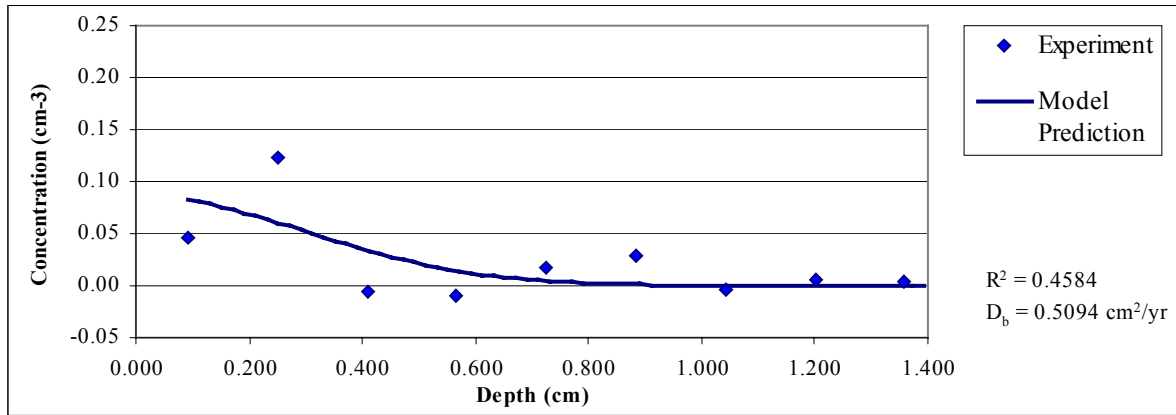


Figure A.7 Model Curve Fit to Core 'A', Experiment 2

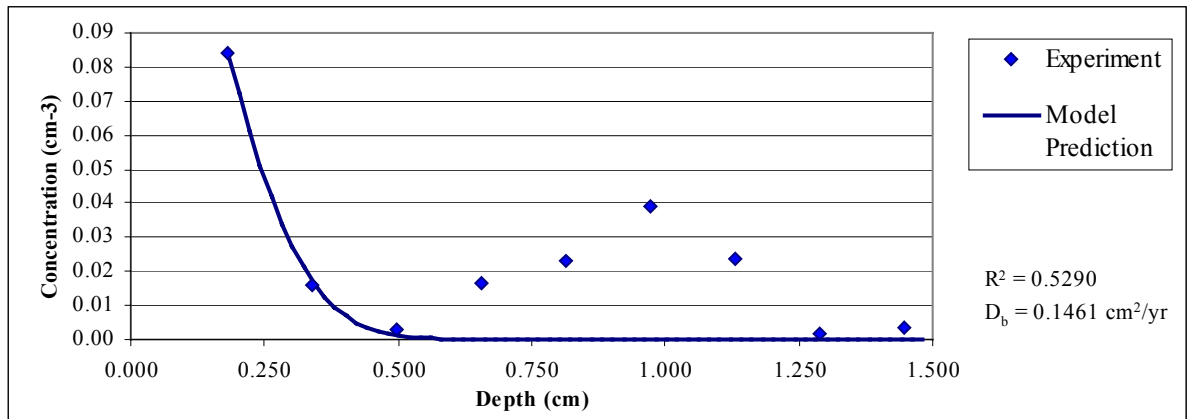


Figure A.8 Model Curve Fit to Core 'B', Experiment 2

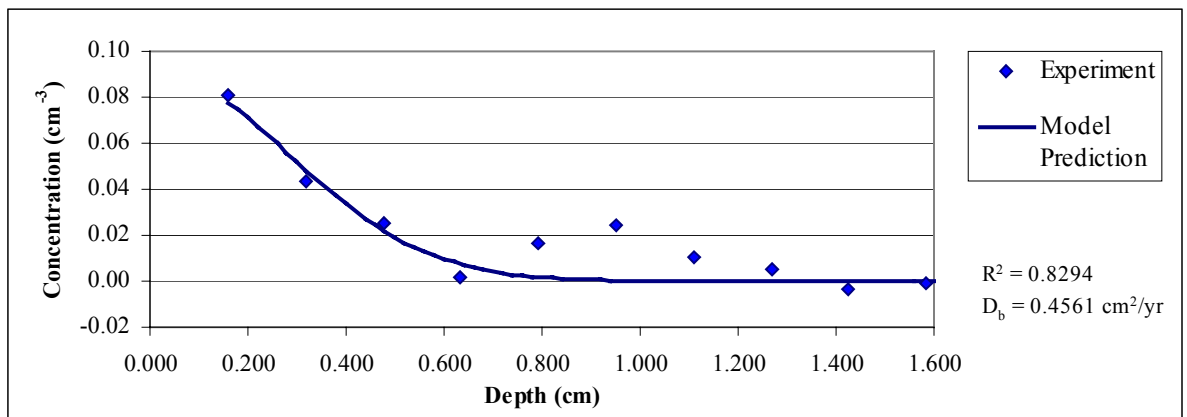


Figure A.9 Model Curve Fit to Core 'C', Experiment 2

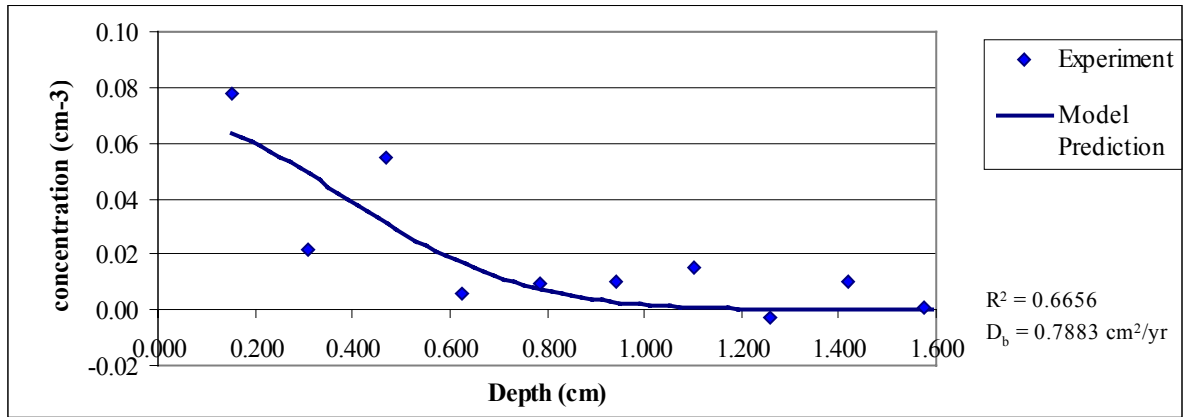


Figure A.10 Model Curve Fit to Core 'D', Experiment 2

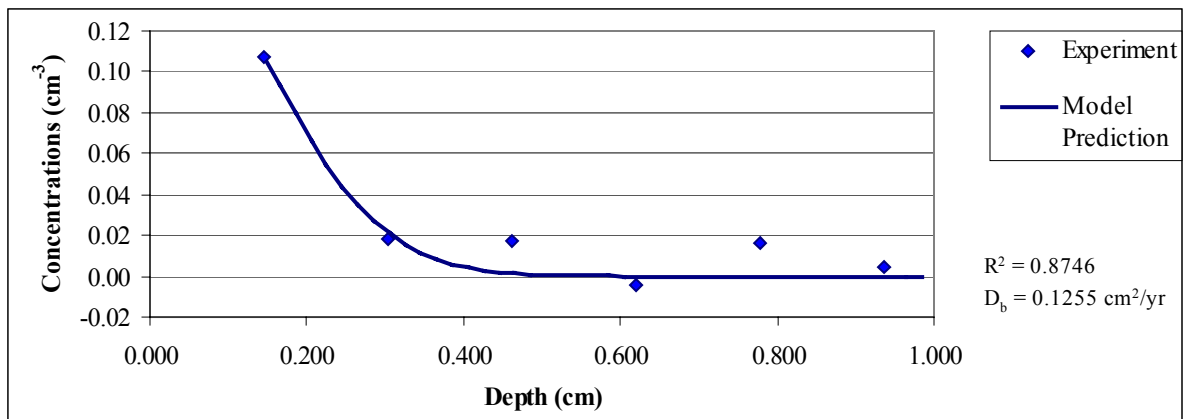


Figure A.11 Model Curve Fit to Core 'E', Experiment 2

A.4.3 Experiment 3, Capitol Lake, February 2002

Table A.9 Raw Data for Experiment 3

Location			Weight of Magnetite (g)				
Slice #	Depth Range (mm)	Average Depth (mm)	Core 'A'	Core 'B'	Core 'C'	Core 'D'	Core 'E'
1	0.000-1.583	0.792	0.019	0.270	0.687	0.108	0.029
2	1.583-3.167	2.375	0.071	0.187	0.238	0.179	0.086
3	3.167-4.750	3.958	0.058	0.250	0.171	0.060	0.175
4	4.750-6.333	5.542	0.071	0.189	0.123	0.017	0.102
5	6.333-7.917	7.125	0.048	0.146	0.037	0.014	0.045
6	7.917-9.500	8.708	0.028	0.086	0.023	0.014	0.023
7	9.500-11.083	10.292	0.009	0.027	0.010	0.014	0.015
8	11.083-12.667	11.875	0.004	0.011	0.007	0.012	0.007
9	12.667-14.250	13.458	0.002	0.004	0.007	0.005	0.003
10	14.250-15.833	15.042	0.001	0.004	0.007	0.001	0.001
11	15.833-17.417	16.625	0.001	0.003	0.007	0.001	0.001
12	17.417-19.000	18.208	0.001	0.002	0.005	0.001	0.001
13	19.000-20.583	19.792	0.001	0.003	0.009	0.001	0.001
14	20.583-22.167	21.375	0.001	0.001	0.003	0.002	0.001
15	22.167-23.750	22.958	0.001	0.001	0.002	0.001	0.001
Total	-	-	0.314	1.177	1.303	0.424	0.485
Loading (g/cm³)	-	-	0.0176	0.0661	0.0731	0.0238	0.0272

Table A.10 Normalized Adjusted Concentrations for Experiment 3

Location			Normalized Adjusted Concentrations (cm ⁻³)				
Slice #	Depth Range (mm)	Average Depth (mm)	Core 'A'	Core 'B'	Core 'C'	Core 'D'	Core 'E'
1	0.000-1.583	0.792	0.0217	0.0815	0.1859	0.0903	0.0212
2	1.583-3.167	2.375	0.0501	0.0256	0.0336	0.1188	0.0532
3	3.167-4.750	3.958	0.0381	0.0475	0.0183	0.0222	0.0999
4	4.750-6.333	5.542	0.0581	0.0342	0.0104	-0.0087	0.0517
5	6.333-7.917	7.125	0.0363	0.0256	-0.0085	-0.0068	0.0144
6	7.917-9.500	8.708	0.0159	0.0099	-0.0098	-0.0044	0.0007
7	9.500-11.083	10.292	-0.0033	-0.0054	-0.0109	-0.0019	-0.0026
8	11.083-12.667	11.875	-0.0059	-0.0072	-0.0086	-0.0004	-0.0054
9	12.667-14.250	13.458	0.0023	0.0012	0.0019	0.0042	0.0022
10	14.250-15.833	15.042	0.0011	0.0012	0.0019	0.0008	0.0007
11	15.833-17.417	16.625	0.0011	0.0009	0.0019	0.0008	0.0007
12	17.417-19.000	18.208	0.0011	0.0006	0.0014	0.0008	0.0007
13	19.000-20.583	19.792	0.0011	0.0009	0.0024	0.0008	0.0007
14	20.583-22.167	21.375	0.0011	0.0003	0.0008	0.0017	0.0007
15	22.167-23.750	22.958	0.0011	0.0003	0.0005	0.0008	0.0007

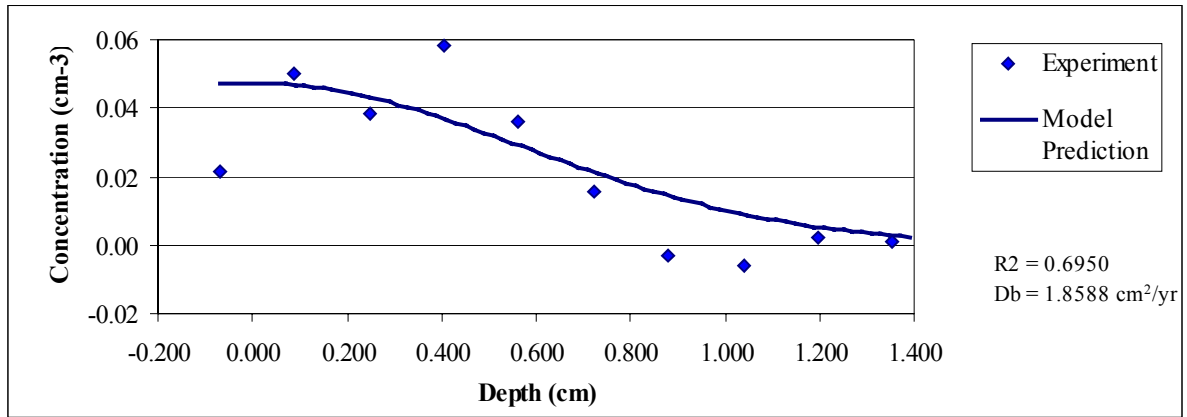


Figure A.12 Model Curve Fit to Core 'A', Experiment 3

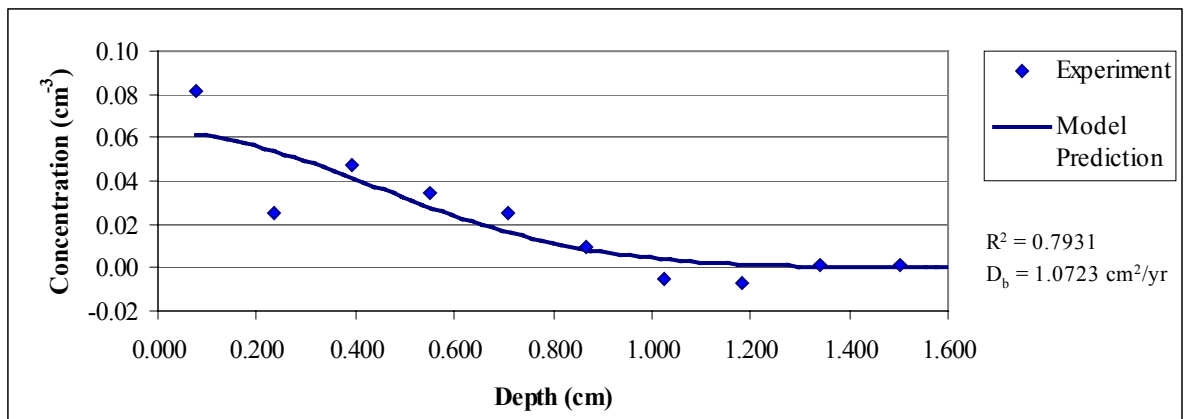


Figure A.13 Model Curve Fit to Core 'B', Experiment 3

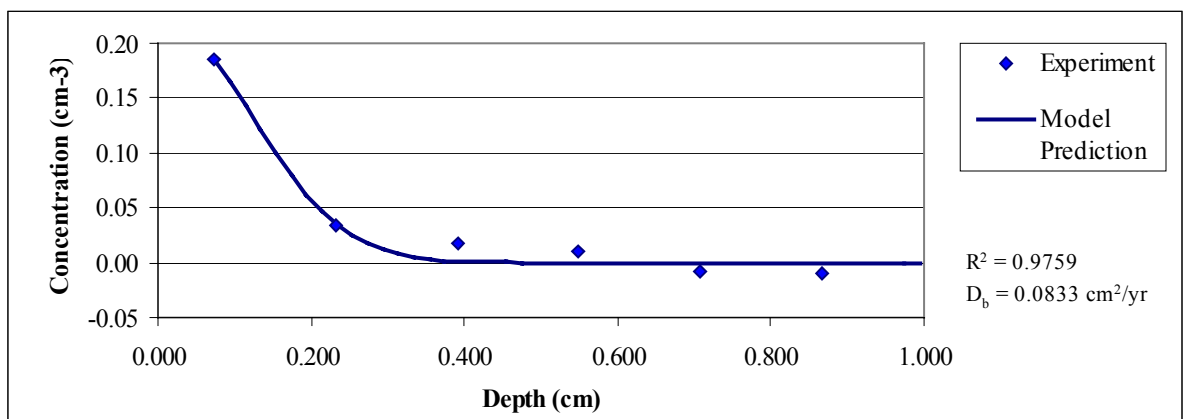


Figure A.14 Model Curve Fit to Core 'C', Experiment 3

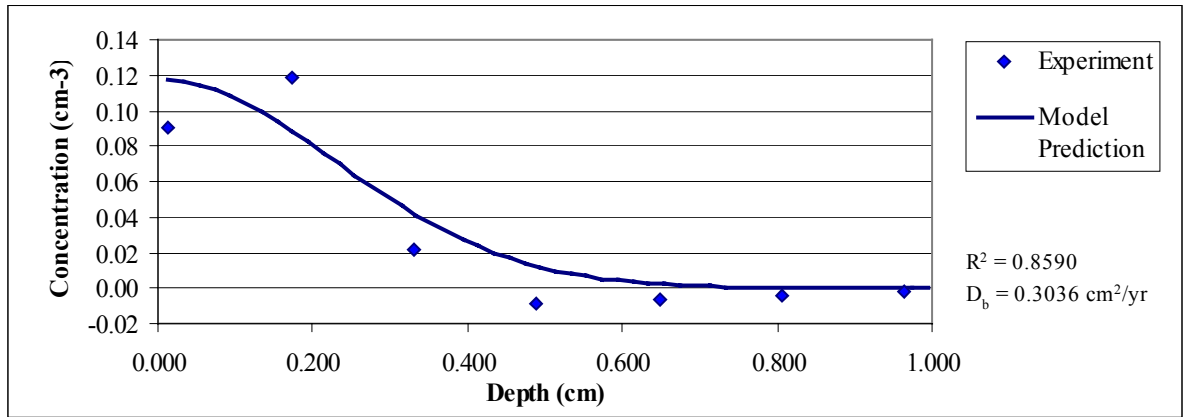


Figure A.15 Model Curve Fit to Core 'D', Experiment 3

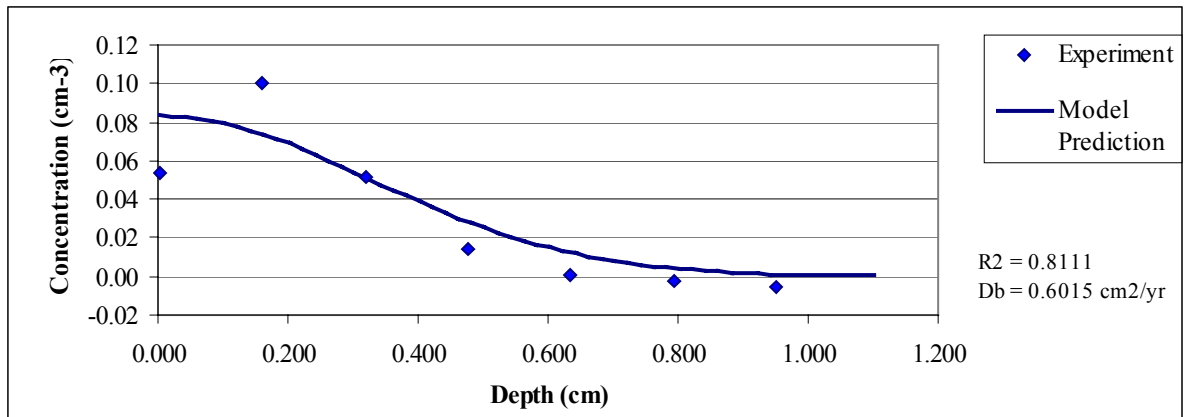


Figure A.16 Model Curve Fit to Core 'E', Experiment 3

Vita

Paul Libbers was born and reared in Baton Rouge, Louisiana, by his parents, David and Elizabeth Libbers. He graduated from Louisiana State University with his Bachelor of Science in Chemical Engineering degree in 1998. Two years later, he returned to Louisiana State University to pursue a Master of Science in Chemical Engineering degree. His interests include contaminated sediment and groundwater remediation, chemical fate and transport modeling, and development of wastewater treatment technology.